Local-density-functional approach to the isostructual γ-α transition in cerium using the self-consistent linearized-augmented-plane-wave method

Warren E. Pickett*
Department of Physics and Astronomy, Northwestern University, Evanston, Illinois 60201

A. J. Freeman
Department of Physics and Astronomy, Northwestern University, Evanston, Illinois 60201
and Argonne National Laboratory, Argonne, Illinois 60439

D. D. Koelling
Argonne National Laboratory, Argonne, Illinois 60439
(Received 4 April 1980)

The isostructural γ-α phase transition of Ce which occurs at 8 kbar has been studied by means of fully self-consistent (non-muffin-tin potential) linearized-augmented-plane-wave energy band calculations carried out for five different values of the lattice constant. In contradiction to the $4f$ electron promotional model of the transition, the results yield essentially one $4f$ electron to be occupied in each phase but with the $4f$ wave function somewhat less localized, and therefore more bandlike, in the "collapsed" α phase. A singly occupied $4f$ state is shown to be consistent with the available experimental data. These results strongly support the picture of a $4f$ localized $\leftrightarrow$ itinerant transition at the γ-α transition and conflict with the promotional model in which some fraction of $4f$ electrons are transferred to the sd conduction bands. The weaker bonding of the $4f$ electrons, compared to that of the $6s$-$5d$ valence electrons, accounts for α-Ce appearing to have 3.5–3.7 bonding electrons in some respects. Calculation of the superconducting transition temperature T_c suggests that a small spin-fluctuation contribution detrimental to superconductivity is necessary to account for the very low value of T_c in α-Ce. Comparison with specific-heat data also suggests a spin-fluctuation contribution to the effective mass; susceptibility data point to a moderate exchange enhancement in α-Ce. We calculate a spin-susceptibility (Stoner) enhancement that increases with temperature, in agreement with experiment up to 150 K, and which tends to diverge at higher temperatures. Certain experiments are suggested which could help greatly in understanding further some important characteristics of the α phase.

I. INTRODUCTION

Cerium, the first element in the rare-earth transition series, is unique among the rare-earth metals. It has a number of unusual properties thought to be associated with the sensitivity to environment of the binding and/or bonding of its single $4f$ electron. In addition, Ce shows both magnetic and superconducting phases; in fact, both magnetism and superconductivity occur in different regions of what may be considered a single crystallographic phase.

The pressure-temperature (PT) phase diagram of Ce, shown in Fig. 1, is unusual in that it displays at least six solid phases, including superconducting phases[1] (α, α' and perhaps the "tetragonal" phase) as well as magnetic phases[2] (β and γ). In addition, the extensively studied isostructural (fcc-fcc) γ-α transition ends in a critical point[3] at 570 K and 20 kbar which is analogous to the well-known liquid-gas critical point. The volume discontinuity at the γ-α transition, which can be as large as 17% toward the lower end, vanishes at the critical point, although a rapid volume change occurs along the extension of the γ-α line to the minimum in the melting curve. Although not usually considered as such, the γ and α phases actually make up a single crystallographic phase.

The γ phase is magnetic (but disordered), having a magnetic moment and susceptibility consistent with a single occupied $4f$ atomic level.[4] The α phase is essentially a paramagnetic metal with an extremely large linear specific-heat term[5] γ. The large value of γ implies a large density of states $N(E_F)$ at the Fermi energy E_F. Nevertheless, α-Ce only becomes superconducting[1] below 50 mK, and then only around 40 kbar.

The γ-α transition and the concomitant loss of magnetic moment is only the most evident conse-

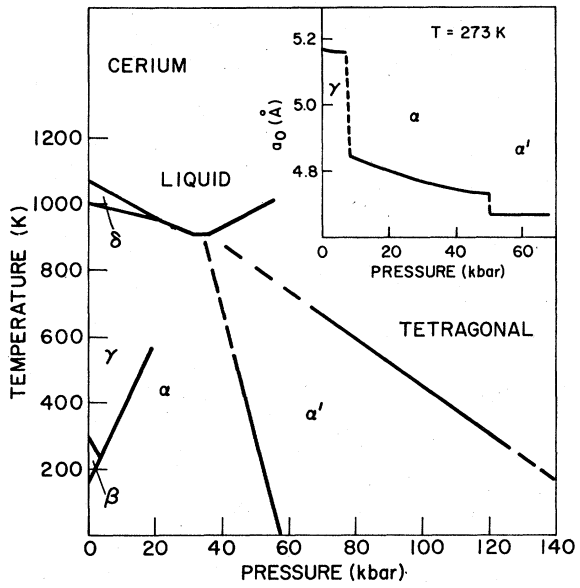

FIG. 1. Idealized pressure-temperature phase diagram of Ce, showing the γ-α transition which ends in a critical point. The inset shows the lattice constant behavior under pressure at 273 K (from Franceschi and Olcese, Ref. 19).

quence of what is apparently a general instability of the Ce $4f$ moment to a reduction of atomic volume. In the $La_{1-x}Ce_x$ system,[6] the pair-breaking influence of the Ce $4f$ moment *increases* in the range $0 < P < 15$ kbar, as the lattice parameter decreases from the La value of ~ 10 a.u. to a value nearer to that of γ-Ce (see Table I). At higher pressures, however, the pair-breaking effect rapidly *diminishes,*[6] signaling the loss of moment upon further reduction of the Ce atomic volume. Similar behavior is found in the[7] $(La_{1-x}Ce_x)_3In$ and[8] $La_{1-x}Ce_xAl_2$ alloy systems. On the other hand, Ce impurities are found to be nonmagnetic in[9] Th, where the atomic volume is about 3% less than that of γ-Ce. In the $Ce_{1-x}Th_x$ alloy system, a critical point occurs[10] at $x = x_c = 0.265$ and $T = 148$ K and the alloy concentration x has been used as a thermodynamic variable similar (but not identical[11]) to the pressure. This extreme sensitivity of the Ce moment may be closely related to the reentrant superconductivity found in the[12] $La_{1-x}Ce_x$, the[13] $La_{1-x}Ce_xAl_2$ and[14] $(La_{0.8}Th_{0.2})_{1-x}Ce_x$ alloy systems.

The γ-α transition was originally suggested[15,16] to be a "valence transition", in which the magnetic localized $4f$ electron is (partially) promoted to the conduction bands, forming an "intermediate valence" phase[17] in α-Ce. This "promotional model" was supported by the interpretation[18] of the atomic volume in terms of nonintegral valency, and by the discovery[19] of the α-α' transition, in which the valence was believed to increase from ~ 3.6 to close to 4. (This latter transition was originally thought also to be isostructural but more recent evidence[20] indicates α'-Ce has the α-U structure.) The promotional model received theoretical support from Coqblin and Blandin,[21] who showed that an Anderson local moment model, with spin compensation by conduction electrons, could lead to a first-order isostructural transition with change of valence if a pressure or temperature dependent f level is postulated. Ramirez and Falicov[22] also showed that a related model system may possess a critical point like that of Ce.

More recently both the "promotional model" and the "intermediate valence" designation have been questioned by a number of workers. The early self-consistent band-structure calculations of Kmetko and Hill[23] indicated a rather similar number of f electrons for the γ and α' phases, which are tetravalent and trivalent, respectively, in the intermediate valence picture. (It is crucial that such calculations be done self-consistently, as it has been shown by various atomic or cellular methods[24] that the occupation number dependence of the $4f$ level is large.) This result was reconciled with the vanishing of the γ-Ce moment by noting that hybridization of the $4f$ state with other states increases with reduction in atomic volume, which then leads to a decreased density of states at the Fermi energy, $N(E_F)$. In the Slater pic-

TABLE I. Input parameters and resulting Fermi energy E_F for Ce at given lattice constants (a): R = APW sphere radius; $a/\sqrt{8}$ = maximum possible APW sphere radius; and E_l = energy about which the lth radial basis function is linearized. Distances are in a.u. (unless otherwise noted) and energies are in Ry.

a	a (Å)	R	$a/\sqrt{8}$	$E_{l\neq 1}$	E_1	E_F
$a_0 = 9.7533$	5.160	3.3850	3.4483	0.5	0.8	0.450
$a_1 = 9.5785$	5.067	3.3850	3.3865	0.5	0.8	0.470
$a_2 = 9.4040$	4.975	3.2808	3.3248	0.6	0.9	0.508
$a_3 = 9.2295$	4.882	3.1799	3.2631	0.6	0.9	0.559
$a_4 = 9.0550$	4.790	3.1799	3.2014	0.6	0.9	0.586

ture of band ferromagnetism, the moment then can become unstable. Kmetko and Hill's interpretation was supported by positron annihilation experiments[25] on the γ, α, and α' phases of Ce which showed no appreciable difference in the number of f electrons in these phases.

Johansson[26] has argued from empirical data that the energy of promotion, from the $f^1(sd)^3$ to the $f^0(sd)^4$ configuration, is much too large to be the driving mechanism in the γ-α transition. He suggests instead that γ-Ce lies on the low-density side of a Mott transition.[27] Under pressure, a $4f$ localization-delocalization transition occurs, with a concomitant loss of moment. Johansson's arguments were not substantiated by any detailed theory, but they contained two attractive features: (1) the f electron number remains nearly unchanged with pressure, with some (possibly small) degree of delocalization, which is consistent with the positron annihilation measurements[25] and the more recent Compton profile measurements[28]; and (2) as no change in symmetry occurs, a critical point in the (P,T) plane is expected.

Another viewpoint, held by Maple and collaborators,[29] favors an Anderson-Friedel local moment instability versus density. This picture contains points in common with both the Mott transition picture of Johansson and the f-sd hybridization picture of Kmetko and Hill. Another point of view is taken by Hirst[30] in the "interconfigurational fluctuation" theory. By assuming that two or more atomiclike configurations lie very close in energy, a number of the anomalies found in Ce can be accounted for.

Other band-structure calculations besides those of Kmetko and Hill have been reported. The earliest were nonrelativistic, non-self-consistent augmented plane wave (APW) calculations by Waber and Switendick,[31] who noted a strong dependence of the f band position on the assumed atomic configuration (or f electron number). They found that a fractional occupancy leads to an approximately consistent result. Mukhopadhyay and Majumdar[32] performed both nonrelativistic and relativistic APW (RAPW) calculations (non-self-consistent) on α- and γ-Ce. They noted a large dependence of the f band position on the assumed exchange-correlation functional as well as on the configuration, and concluded that self-consistency must be included to make further progress in understanding the electronic structure of Ce. Rao *et al.*[33] used a non-self-consistent relativistic Korringa-Kohn-Rostoker (KKR) method to study dhcp β-Ce, but concluded that the f states, which were found to lie well above E_F and to be nearly unoccupied, were not described well by their calculations. Glötzel and Fritsche[34] reported non-self-consistent semirelativistic rigorous cellular method results for γ- and α-Ce, but no f electron occupation number was given. Finally, Glötzel[35] reported a number of results from self-consistent relativistic linear muffin-tin orbital (LMTO) calculations within the atomic sphere approximation (ASA) and found 1.2 f electrons in α-Ce, consistent with the ideas of Johansson and similar to the results of Hill and Kmetko. The f electron number increased only slightly under pressure. In addition, a ferromagnetic instability was found at approximately the γ-Ce lattice constant. This result could be very important in establishing the itinerancy of f electrons in α-Ce and thereby the validity of the band approach for Ce.

The validity of the "band-structure approach" for describing the $4f$ electrons has been strongly questioned since the early pioneering band-structure studies of the rare earths by Freeman and Dimmock.[36] These authors, Waber and Switendick[31] and, more recently, Sinha and Fedro[37] have suggested that, *in the study of excited state properties,* the otherwise applicable Fermi-Dirac statistics should be modified to account for the large occupation number dependence of the $4f$ levels. The foundations of density functional theory (which is the only "band-structure approach" which we will discuss), set forth by Hohenberg, Kohn, and Sham, establish that for *ground-state properties* self-consistency is to be carried out on the one-electronlike states using Fermi-Dirac statistics (at zero temperature). It should be noted that the local density approximation to the exchange-correlation functional is not the principal issue here, although $4f$ band materials have not been studied extensively by this approach to date. What is at issue is the interpretation of eigenvalue differences in relation to excited states, and when highly excited $4f$ states are involved, it is clear that corrections are necessary.[24] Waber and Switendick,[31] and more recently Sinha and Fedro,[37] have proposed specific methods which may prove useful in describing excited states. Part of the motivation of this study of the electronic structure is to determine in which cases corrections are necessary to describe the excited states and thermodynamics of Ce.

The relation between the pressure behavior of Ce and the variation of properties across the entire series of actinide metals also provided impetus for the present investigation. In the actinides, a concept of central interest concerns the importance of $5f$ bonding with respect to the transition from itinerant to localized states across this series. For the more localized $4f$ states, the corresponding transition may occur entirely within Ce, in the range of accessible pressures if not at the γ-α transition itself. The probable occurrence of the α-U structure in Ce at high pressure,[20] which is believed to occur in the actinides because of strong and complicated itinerant $5f$ bonding, further suggests the model of Ce as the $4f$ analog of the itinerant-to-localized $5f$ transition.

In this paper, we apply a general form of local density functional theory to study the electronic proper-

ties of fcc Ce for a range of atomic volumes between that of γ-Ce and α-Ce. The results we describe are obtained from fully self-consistent (SC) (i.e., non-muffin-tin) relativistic, linearized APW (LAPW) calculations. The calculations are restricted only to paramagnetic systems and a charge density and potential consistent with the cubic site symmetry. Thus, e.g., ferromagnetism and atomiclike configurations with symmetry lower than cubic are not considered.

The method of calculation, together with approximations and convergence criteria, are discussed in Sec. II. The resulting band structures, charge densities and potentials are presented in Sec. III and compared with previous calculations. Where possible, comparison with experiment is made. The electron-phonon interaction λ and superconducting transition temperature T_c are studied within the rigid muffin-tin approximation in Sec. IV, where it is shown that theoretical values of λ and T_c are small in spite of an extremely large density of states $N(E_F)$. A discussion of the present theoretical understanding of γ-Ce and α-Ce is given in Sec. V.

II. METHOD OF CALCULATION

Since detailed discussions of our calculational procedures have been given elsewhere,[38–41] only a descriptive review will be presented here. This will serve to orient the reader and to provide a basis for discussing discrepancies between the present results and those obtained previously by other means. The discussion is separated into three parts: (i) the secular equation and its solution; (ii) the determination of the charge density and resulting screening potential necessary for the self-consistency loop; and (iii) the treatment of the spin-orbit interaction at the final step.

A. Secular equation

Ideally one would like to solve the Dirac equation for a relativistic electron in a periodic potential V. The basis set $\{\Phi\}$ is constructed in the usual APW dual representation,[41] as plane waves outside non-overlapping spheres of radius R and as solutions of a spherically averaged potential V_0 inside the spheres. This results in coupled first-order differential equations for the radial functions g_κ, f_κ, in terms of which the basis APW is given by[41] (in standard notation)

$$\Phi_{\kappa\mu}=\begin{pmatrix} g_\kappa \chi_{\kappa\mu} \\ -i f_\kappa \sigma_r \chi_{\kappa\mu} \end{pmatrix}, \quad r<R \quad . \tag{1}$$

Here κ, μ are the relativistic quantum numbers for the central field problem and g (f) is the radial function describing the large (small) component. For each value of the nonrelativistic orbital quantum number l, there are two values of κ corresponding to total angular momentum $j=l+\frac{1}{2}$ and $j=l-\frac{1}{2}$.

Koelling and Harmon[38] have shown that in many cases it is desirable to retain spin as a "good" quantum number, both for computational and physical reasons. This can be done by forming a j-weighted average g_l, for a given l, of the radial solutions g_κ, and subsequently dropping a κ-dependent term in the differential equation for g_κ which corresponds to spin-orbit coupling. In effect this reduces the solution of the radial problem to the simplicity of the corresponding nonrelativistic problem while including the important Darwin and mass-velocity corrections. The spin-orbit interaction, in addition to being generally smaller, serves primarily to split degenerate states (or states of similar l character) at points, or along lines, of high symmetry. The spin-orbit corrections are often negligible; for Ce, however, they have been included in a final variational procedure, described in Sec. II C below.

The energy-dependent secular equation is linearized following Koelling and Arbman.[39] The radial solution $g_l(E)$ is replaced by a linear combination of the solution $g_l(E_l)$ at a fixed energy E_l and the energy derivative $g_l(E_l)$, also evaluated at E_l. The linear combination is fixed by requiring both the basis function and its derivative to be continuous across the sphere boundary. The resulting technique has been found to be quite accurate (see below) over a range of several tenths of a Rydberg around $E=E_l$. In Table I the input parameters for the calculations for Ce are presented.

The periodic potential $V(r)$ is restricted only to have a form consistent with the symmetry of the crystal. For Ce, it is expanded, in the unit cell at the origin, in the dual representation

$$V(\vec{r})=\begin{cases} \sum_{\vec{K}} V_{\vec{K}} e^{i\vec{K}\cdot\vec{r}}, & r>R \\ \sum_{l} V_l(r) K_l(\hat{r}), & r<R \end{cases} \quad . \tag{2}$$

Here K_l denotes the Kubic harmonics of full cubic (Γ_1) symmetry, and only the $l=0$, 4, and 6 harmonics are retained. Higher l harmonics are expected to give negligible corrections. The Fourier expansion in the interstitial region is carried to far more reciprocal lattice ($\vec{K}$) stars (90) than is actually necessary for convergence. Using these criteria, the truncation of these representations leads to a maximum discontinuity in V at the sphere radius of 35 mRy for Ce. The anisotropy for α-Ce was 210 mRy, which was the difference in V along the (100) and (110) directions at the sphere radius.

The crystal eigenfunctions are expanded as a linear

combination of the LAPW basis functions with the coefficients being determined variationally. In addition to the usual kinetic energy and spherical potential energy matrix elements, it is necessary to calculate the matrix elements of warping and nonspherical terms in the potential in Eq. (2). The procedure is straightforward and has been described elsewhere.[41]

It only remains to fix the number of basis functions to be used in the secular equation. This is done separately for each k point by including all LAPW's corresponding to the condition $|\vec{k}+\vec{K}| < K_{\max}$. To get reasonable convergence of the f bands (see below) we find $RK_{\max}=8$ to be a useful criterion, corresponding to ~ 55 LAPW's. For $RK_{\max} \geq 9$ (corresponding to 70–80 LAPW's) approximate linear dependence of the basis set can sometimes lead to numerical difficulties in the Choleskii decomposition of the overlap matrix.

B. Construction of the general potential

The charge density ρ is expanded in a straightforward manner in a dual representation in parallel with the potential and the basis functions, again retaining $l=0$, 4, and 6 Kubic harmonic terms inside the sphere. This charge density is used to construct the screening potential, consisting of the electrostatic potential which satisfies Poisson's equation and an exchange-correlation potential in the local density approximation. All the results described here were obtained using the Kohn-Sham-Gaspàr $(\alpha=\frac{2}{3})\rho^{1/3}$ approximation, with no explicit additional correlation correction. Using a correlation potential corresponding to a (perhaps density dependent) α greater than $\frac{2}{3}$ would lead to slightly more localized f states.

The grid of k points used to calculate ρ consisted of equally weighted points at the center of mass of 16 equal volume tetrahedra in the irreducible Brillouin zone (IBZ). None of these points lie on symmetry directions so the possible problem of degenerate states at E_F never arises. For α-Ce, each tetrahedron was subdivided into eight equal volume tetrahedra, and the centers of mass of these (128 equally weighted) tetrahedra made up its final k-point grid. The differences between the 16 and 128 k-point results (mainly some minor changes in the nonspherical densities ρ_4 and ρ_6) were not large enough to warrant the more exacting self-consistency criterion for the other four lattice constants.

C. Spin-orbit interaction

The spin-orbit (SO) interaction was ignored (as described in Sec. II A) in the iterations to self-consistency. This is a reasonable approximation in most systems since the effect of SO corrections is primarily to split degeneracies along symmetry lines rather than to cause a net shift of states to higher or lower energy. However, in Ce the SO corrections are important for certain properties, as will be discussed below.

The observation that the SO interaction only splits degeneracies suggests an approach in which SO is treated in a separate variation within a subset of bands, which in practice will consist of only the bands in the energy region of interest (near E_F). This method has been discussed in detail elsewhere[40] so only a descriptive review will be given here.

Suppose the $N \times N$ secular equation described in Sec. II A has been solved for the lowest M eigenstates $(M < N)$—a common numerical practice to save computational time when all eigenstates are not desired. For Ce, the region of interest includes s (1), d (5), f (7), and perhaps p (3) bands, so that $M \simeq 15$. (Recall that $N \approx 60$ has been used for the secular equation.) Within this M subspace, the SO matrix elements are evaluated and the effective Hamiltonian is rediagonalized yielding approximate (but usually excellent) fully relativistic eigenstates and eigenvalues.

The advantage of this procedure is that spin is retained as a good quantum number as long as possible. This is preferable physically, of course, but also is computationally very desirable, since it is only necessary to handle a $2M \times 2M$ (30×30) complex matrix in the final stage rather than a $2N \times 2N$ $(120 \times 120$ in this case) complex matrix throughout the SC procedure.

This scheme has been found to be very accurate for determining eigenvalues in Ce and La (Ref. 42) as well as in transition metals.[40] The primary restriction seems to be that the resulting relativistic eigenfunctions are required, for a given l, to have the same radial dependence for $j = l \pm \frac{1}{2}$; i.e., there is only one radial function g_l for each l rather than the two functions g_κ from the full relativistic treatment. This restriction may be more serious in very heavy elements.[40]

To include the SO interaction in the LAPW method it is necessary to evaluate the quantities[40]

$$\xi_l^0 = \int_0^R dr\, r^2 \left(\frac{g_l}{2Mcr}\right)^2 r\frac{dV}{dr} \ , \tag{3a}$$

$$\xi_l^1 = \int_0^R dr\, r^2 \left(\frac{g_l}{2Mcr}\right)\left(\frac{\dot{g}_l}{2Mcr}\right) r\frac{dV}{dr} \ , \tag{3b}$$

$$\xi_l^2 = \int_0^R dr\, r^2 \left(\frac{\dot{g}_l}{2Mcr}\right)^2 r\frac{dV}{dr} \ , \tag{3c}$$

which provide the magnitude of the SO interaction $\xi_l(E)$

$$\xi_l(E) \cong \xi_l^0 + 2(E-E_l)\xi_l^1 + (E-E_l)^2\xi_l^2 \ . \tag{4}$$

TABLE II. Values of the spin-orbit parameters defined in Eqs. (3) and (4), in mRy units. The lattice constants are given in Table I.

		ξ_l^0	ξ_l^1	ξ_l^2	$\xi_l(E_F)$
	a_0	50.5	−6.4	0.8	55.1
	a_1	50.9	−6.7	0.9	55.4
$l=1$	a_2	57.5	−7.7	1.0	63.7
	a_3	66.9	−9.9	1.5	73.9
	a_4	67.6	−10.2	1.6	74.2
	a_0	3.3	2.3	1.6	3.1
	a_1	3.2	2.2	1.5	3.1
$l=2$	a_2	3.7	2.3	1.4	3.3
	a_3	3.6	2.1	1.2	3.5
	a_4	3.5	2.0	1.1	3.5
	a_0	3.6	3.4	3.2	3.3
	a_1	3.5	4.0	4.8	3.3
$l=3$	a_2	3.8	2.2	1.3	3.4
	a_3	3.5	3.5	3.5	3.2
	a_4	3.3	3.8	4.5	3.2

In Eq. (3), dV/dr is the radial derivative of the spherical part of the potential and $2M = 2m + (E_l - V)/c^2$. The resulting values for Ce at three lattice constants are given in Table II up to $l=3$; for higher l, the ξ_l^j are less than 5×10^{-6}. The $l=1$ SO parameter is large (~ 55 mRy) but enters into eigenvalues in the region of interest with negligible weight because the wave functions have very little p character. Note that the spin-orbit parameter at the Fermi energy increases with decreasing atomic volume [to within the accuracy of the expansion of Eq. (4)]. This is consistent with the electron spending a greater time near the nucleus as the volume is reduced.

III. CALCULATIONAL RESULTS

A. Band structure and density of states

The band structures of γ-Ce and α-Ce, from the bottom of the s band to the top of the d bands, are shown in Figs. 2 and 3, respectively. The spin-orbit interaction has been included in the eigenvalues plotted here to provide a clear indication of the size and importance of SO corrections. However, since the SO effects are rather small (although sometimes important), it is more transparent physically to present, as much as possible, the discussion in terms of the corresponding band structures before including the SO interaction. This also facilitates comparison with other calculations which neglect the SO interaction.

Throughout the range of atomic volumes we have studied, the band structure is characterized by wide (~ 10 eV) d bands, typical of an early fcc $5d$ transition metal, and by narrow $4f$ bands (~ 1 eV), to the bottom of which E_F is "pinned" (see below). The behavior of the eigenvalues at the Γ and X points under reduction of atomic volume is shown in Fig. 4. The s state Γ_1 rises monotonically relative to E_F, and the d and f bands broaden monotonically. The difference in f-band widths as determined from eigenvalues at the zone center Γ and $X = (2, 0, 0)$ (π/a) is apparent. In fact, from Figs. 2 and 3 it can be seen that the f bands are narrow and dispersionless in a

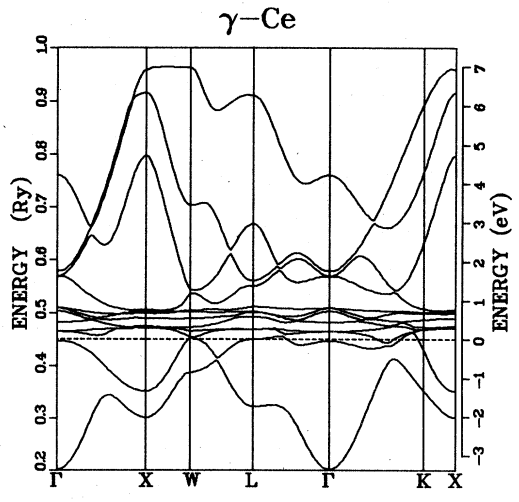

FIG. 2. Self-consistent band structure, including the spin-orbit interaction, for γ-Ce. The Fermi energy E_F lies near the bottom of the flat $4f$ bands. The energy scale on the left is relative to the average interstitial potential.

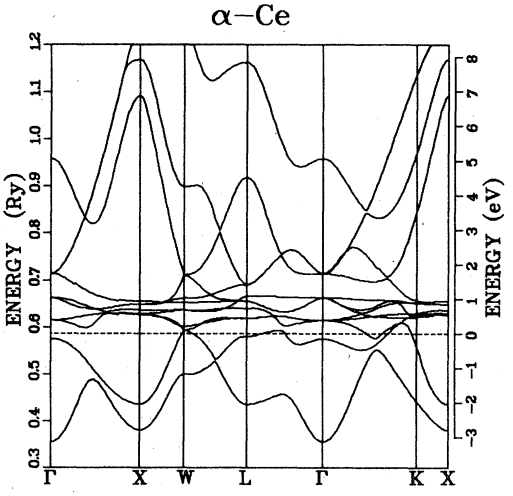

FIG. 3. Same as Fig. 2, but for α-Ce.

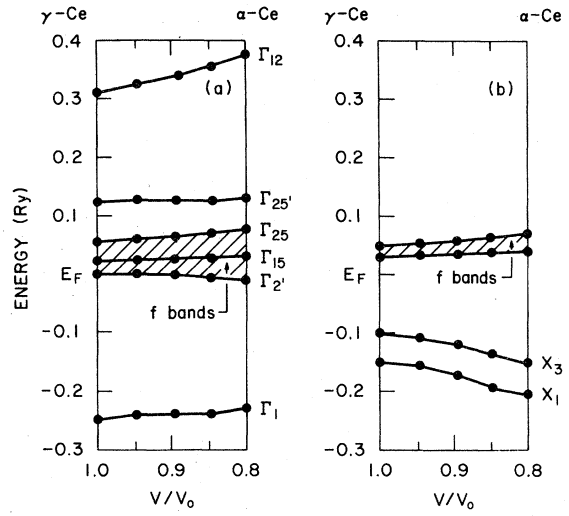

FIG. 4. Behavior of eigenvalues at Γ and X under reduction of atomic volume. The filled circles represent the calculational results at the five lattice constants listed in Table I.

certain volume surrounding the X point. This effect was also found in La, where it also became clear that the Γ point is most appropriate for determining an f-band width, W_f. (The d-band width, W_d, is conventionally defined by eigenvalues at the X point, for example.) There is more than a *60% increase* in W_f in going from γ-Ce to α-Ce [$W_f \equiv E(\Gamma_{25}) - E(\Gamma_{2'})$ here]. The corresponding d-band width increase is 40–45%. The center of the f bands (relative to E_F) C_f, defined by the mean of the f eigenvalues at Γ (respectively, X), increases from 33 to 44 mRy (respectively, 38 to 53 mRy).

The effects due to including the SO interaction in a final variation are shown in Table III, where eigenvalues at Γ and X, with and without SO interaction included, are presented for γ-Ce and α-Ce. Our procedure for including SO effects was found to reproduce fully relativistic APW eigenvalues to better than 1 mRy in Pd and 4 mRy in Pt. An interesting and potentially important effect of the SO interaction is to increase W_f significantly, from 54 to 62 mRy for γ-Ce and from 88 to 92 mRy in α-Ce. The Fermi surface can also be sensitive to SO corrections, since the bands are very flat and eigenvalues near E_F can be shifted by as much as 5 mRy. The Fermi surface will be discussed in more detail below. As can be seen from ξl in Table II, the spin-orbit corrections for

TABLE III. Eigenvalues (mRy), at Γ and X in γ-Ce and α-Ce, showing the effect of including the spin-orbit (SO) interaction. The symmetry labels at Γ are indicated, and numbers in parentheses denote degeneracy when spin-orbit corrections are included. The Fermi energy is 450 mRy for γ-Ce and 586 mRy for α-Ce.

	Γ				X			
	γ-Ce		α-Ce		γ-Ce		α-Ce	
	no SO	SO	no SO	SO	no SO	SO	no SO	SO
Γ_1	203	203	356	356	302	302	381	381
$\Gamma_{2'}$	450	447	575	574	352	352	436	436
Γ_{15}	473	465(2)	615	607(2)	480	472	626	621
		483		624		472	629	622
Γ_{25}	504	503	663	661	483	475		622
		509(2)		667	484	490	635	640
$\Gamma_{25'}$	573	569(2)	714	710(2)	494	499	648	650
		579		721		502		656
Γ_{12}	760	760	958	958	500	506	655	659
					797	795	1091	1092
					917	916	1169	1169
					964	959		
						971		

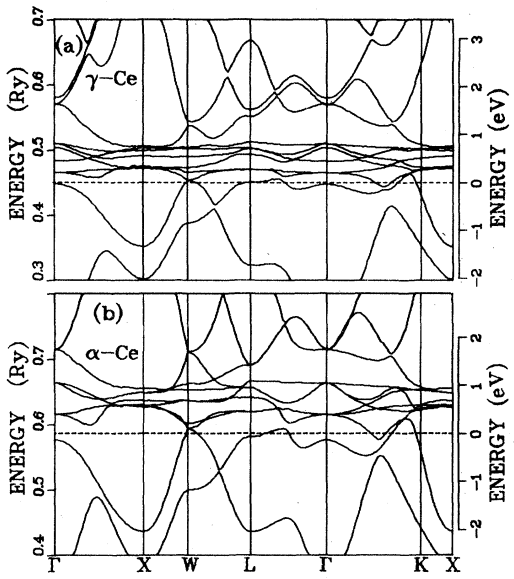

FIG. 5. The 4*f*-band region of the band structures of (a) γ-Ce and (b) α-Ce. As in Figs. 2 and 3, these bands are plotted directly from the first principles eigenvalues at 180 closely-spaced points. The small kinks result from a lack of convergence which is discussed in the text.

f bands are not very sensitive to atomic volume in the range we have studied.

Figure 5 shows the *f* bands in γ-Ce and α-Ce on an enlarged scale. These plots, as do those of Figs. 2 and 3, result directly from a graphic program using 180 closely-spaced first-principles *k* points. The small kinks in the plots reflect a lack of convergence of the eigenvalue ($\lesssim 5$ mRy) on the high side of the kink. In principle, these kinks can be eliminated by increasing the number of APW's (~ 55) in the basis. Unfortunately, numerical instabilities arise in the Choleskii decomposition of the overlap matrix if the basis is increased. Thus it would be necessary to utilize more sophisticated matrix routines to produce more precisely converged bands. Note that the kinks appear only in the *f* bands which are the most difficult to converge using a plane-wave basis. (The problem may arise from approximate linear dependence when expanding $l=3$ wave function in augmented plane waves.) The resulting lack of convergence in the eigenvalues, and especially the eigenfunctions, make it questionable to what extent self-consistency on the 128 *k*-point grid (used only for α-Ce) can be expected to be superior to the less stringent 16 *k*-point self-consistency.

For two phases which show such different physical properties, the band structures of γ-Ce and α-Ce shown in Fig. 5 are quite similar. The primary effect is a general broadening of the bands. Since the Fermi level is effectively pinned to the bottom of the *f* bands, the broadening of the *f* bands means that the *f*-band center must rise relative to E_F. Under this 20% reduction in volume, no band orderings change, and with the exception of the second band near the *L* point, the intersections of the Fermi surface with the *symmetry directions* of Fig. 5 show surprisingly little change. Band 2 at *L*, which is at E_F in γ-Ce, drops to -7 mRy in α-Ce. The other noticeable difference in Fig. 5 is at Γ, where the Γ_2-derived *f* state, which lies at -3 mRy in γ-Ce, falls to -12 mRy in α-Ce. The effects of these changes, as well as other changes off symmetry directions, on the Fermi surface will be described below.

The broadening of the bands under pressure is also evident in Fig. 6, where the total density of states for γ-Ce, α-Ce, and an intermediate lattice constant are

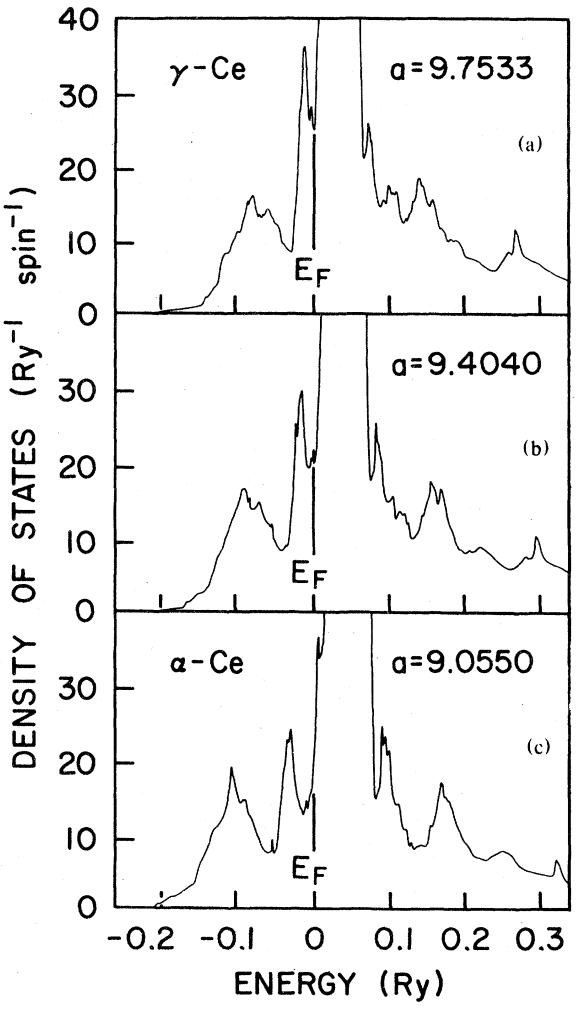

FIG. 6. The density of states of (a) γ-Ce, (b) an intermediate lattice constant, and (c) α-Ce. The broadening of all the bands under the reduction of volume can be seen here. The Fermi energy E_F falls at or near a minimum, nevertheless $N(E_F)$ is very large.

TABLE IV. Angular momentum decomposed muffin-tin density of states at E_F, $N_l(E_F)$, and corresponding charges Q_l. For d and f contributions, the specific irreducible representations are given. The lattice constants $a_0, \ldots, a_4$ are given in Table I.

		s	p	$d(\Gamma_{25'})$	$d(\Gamma_{12})$	$f(\Gamma_{2'})$	$f(\Gamma_{25})$	$f(\Gamma_{15})$	g	Int.	Total
	a_0	1.0	1.3	4.8	2.2	6.1	7.6	26.9	0.05	5.1	55.1
	a_1	1.2	1.3	4.8	2.0	5.2	7.6	22.8	0.06	4.1	49.1
$N_l(E_F)$	a_2	1.1	1.0	3.9	1.7	4.3	7.0	18.6	0.05	4.0	41.7
$(\text{eV atom})^{-1}$	a_3	1.0	0.9	3.4	1.4	3.4	6.0	13.4	0.04	3.8	33.4
	a_4	1.3	0.9	3.4	1.3	2.9	6.6	11.9	0.05	3.2	31.6
	a_0	0.38	0.16	0.95	0.55	0.34	0.14	0.53	0.005	0.94	4.000
	a_1	0.38	0.17	1.00	0.58	0.35	0.14	0.58	0.006	0.79	4.000
Q_l	a_2	0.34	0.15	0.99	0.57	0.34	0.16	0.60	0.006	0.84	4.000
	a_3	0.31	0.14	0.97	0.57	0.33	0.16	0.59	0.006	0.92	4.000
	a_4	0.31	0.14	1.02	0.60	0.33	0.17	0.61	0.007	0.81	4.000

shown. The density of states was calculated with the tetrahedron method, using 1024 tetrahedra in the IBZ. First principles eigenvalues were calculated at the vertices of each tetrahedron (totaling 293 distinct points) and the energy was interpolated linearly within each tetrahedron. This procedure results in sufficiently accurate results with modest computational effort and eliminates uncertainties which arise from the use of Fourier series representations.

The Fermi level is found in each case to lie at the bottom edge of the huge peak arising from the flat f bands. Due to the band broadening, $N(E_F)$ decreases from 27.5 states/Ry spin in γ-Ce to 15.8 states/Ry spin in α-Ce. To facilitate a more complete description of the electronic structure of Ce, the angular-momentum projected partial density of states, $N_l(E)$, inside the spheres was also computed through $l=4$. The d and f components were also decomposed according to the cubic irreducible representations ($\Gamma_{12}, \Gamma_{25'}$) and ($\Gamma_{2'}, \Gamma_{15}, \Gamma_{25}$) for $l=2$ and $l=3$, respectively. The integral of the occupied partial density of states in turn gives the amount of charge Q_l inside the sphere with a particular angular-momentum character. The "interstitial density of states" can be defined as $N_{\text{int}}(E)=N(E)-\sum_l N_l(E)$, and similarly for the interstitial charge Q_{int}. These quantities have been listed in Table IV, and the behavior of the s, p, d, and f charges Q_l upon reduction in volume are pictured in Fig. 7.

A very important result, which is clearly visible in Fig. 7, is that the f electron number increases only slightly, from 1.01 to 1.11 electrons, in going from γ-Ce to α-Ce. This slight increase is at the expense of the s-p electrons, whose band center rises relative to the f bands under a decrease in volume. The small structure in the d charge Q_2 is primarily a result of changes in the ratio of the muffin-tin volume to the atomic volume, which was not kept fixed as the lattice constant was varied (see Table I). The constancy of the f occupation number has important implications for the applicability of various models of Ce, as will be discussed in the last section.

Understanding the character of the f states is crucial to uncovering the driving mechanism for the γ-α transition discussed in Sec. I. Figure 8 shows the f density of states for γ-Ce and α-Ce, decomposed into contributions from each of the cubic irreducible representations $\Gamma_{15}[z(5z^2-3r^2)]$, $\Gamma_{25}[z(x^2-y^2)]$, and $\Gamma_{2'}(xyz)$. A number of indications of the f electron character can be deduced from Fig. 8. First, the broadening and rising of the center of the

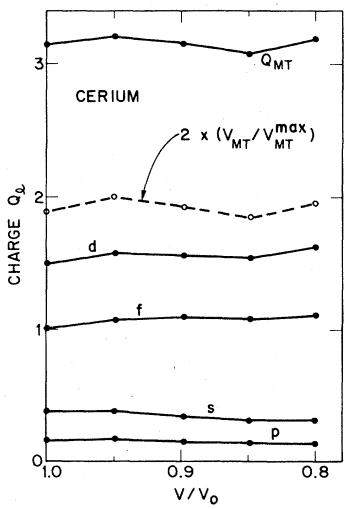

FIG. 7. The behavior of the angular momentum decomposed charge Q_l (filled circles) inside the muffin-tin vs volume V. The volume V_0 corresponds to γ-Ce, $V=0.8\ V_0$ corresponds to α-Ce. Note especially that the f charge is nearly constant. Much of the small d and f variation results from the nonconstant fraction of unit cell volume V_{MT}/V_{MT}^{max} inside the muffin tin shown as open circles.

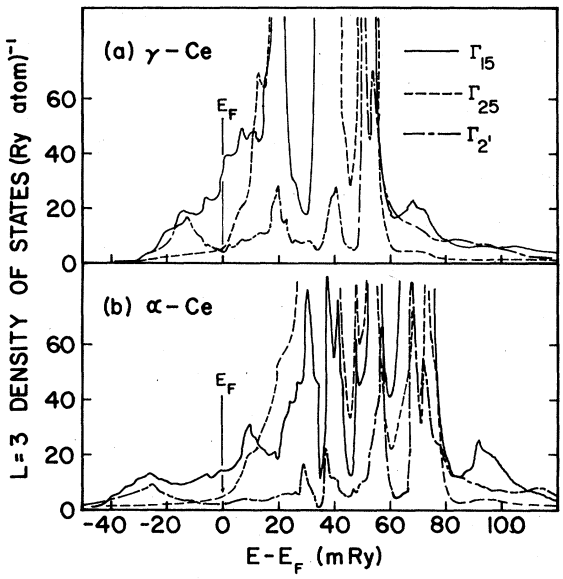

FIG. 8. The $l=3$ density of states inside the muffin tin for (a) γ-Ce and (b) α-Ce. The contribution from each of the cubic irreducible representations Γ_{15}, Γ_{25}, and $\Gamma_{2'}$ is shown separately.

bands is obvious. It is also clear that hybridization increases considerably in going to the α phase, resulting in much longer tails in the f density of states, both above and below the main f band region where the density of states is very large. Furthermore, the density of f states at E_F, which is mostly Γ_{15}-like, is twice as large in γ-Ce, and it is not hard to imagine that this difference could account at least partially for the magnetism of γ-Ce.

It can also be seen from Fig. 8 that the Γ_{25} f states are more dense in the lower half of the bands, the Γ_{15} f states are denser in the upper half, and the $\Gamma_{2'}$ f state peak lies at the top of the f bands. This is just the opposite of what would be expected from examining the f eigenvalues at Γ, which are $\Gamma_{2'}$, Γ_{15}, and Γ_{25} in increasing order (Table III). By examining eigenvalues at zone-boundary points, however, it is found that the f character is inverted with respect to that at Γ. As the zone-boundary regions are weighted more heavily than the zone center, the density of states does not resemble what would be expected from eigenvalues at Γ.

It is clear that the f-band width arises from direct f-f interactions, since both the top and bottom of the f bands occur at Γ where hybridization with s and d states is forbidden by symmetry. This can be substantiated by considering the $4f$ spherical radial charge density at the Fermi energy as shown in Fig. 9 for all five lattice constants studied. The radial density shape, which at first sight appears to be constant, actually changes substantially from γ-Ce to α-Ce in the critical region midway between atoms. Simple considerations suggest that the width of "pure" or "canonical" f bands (i.e., those obtained by disregarding other partial waves) should be proportional to $[g_3(R)]^2$, where R is the midpoint between adjacent atoms. From the inset of Fig. 9 $[g_3(R)]^2$ is seen to increase by 40% in going from γ-Ce to α-Ce. This correlates well with the corresponding increase in bandwidth from 54 to 88 mRy (or 62 to 93 mRy when including the spin-orbit interaction, which is unaffected by density changes as expected).

The nonspherical components ρ_4 and ρ_6 of the Ce charge density, shown in Fig. 10, provide information on bonding, and on the possible contribution of $4f$ states to bonding. The sign and relative magnitude of the Kubic harmonics K_4 and K_6 are also indicated in Fig. 10. It should be noted that only f states contribute significantly to ρ_6, while both d and f states are important in determining ρ_4. The evidence indicates the f states are somewhat antibonding, or at least nonbonding: the charge density contribution $\rho_6 K_6$ is negative along the nearest-neighbor direction and positive along the other two high-symmetry directions. This, of course leads to $Q_{f(\Gamma_{15})}$ and $Q_{f(\Gamma_{2'})}$ (see Table IV) being larger than $Q_{f(\Gamma_{25})}$; the latter points more toward nearest neighbors. In addition K_4 has no lobe along the nearest-neighbor direction. As a result, the charge density shows a tendency to build up in the [111] direction rather than the [110] nearest-neighbor direction as would be required

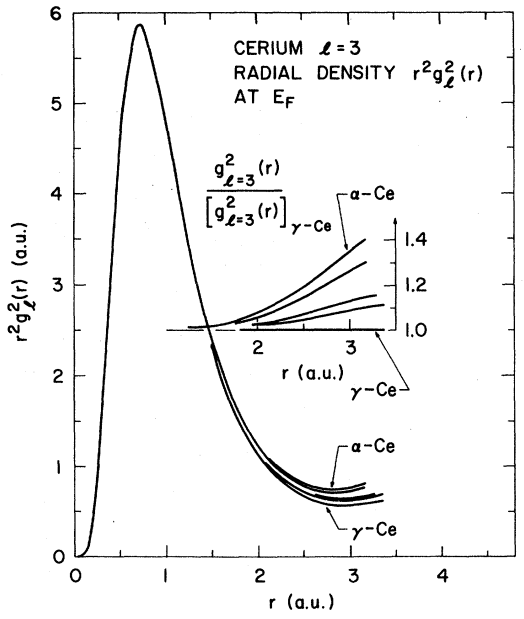

FIG. 9. The radial $l=3$ ($4f$) density at E_F for each of the lattice constants in Table I. The f-f overlap is proportional to g^2 at the muffin-tin radius; the 40% increase in the overlap is demonstrated in the inset.

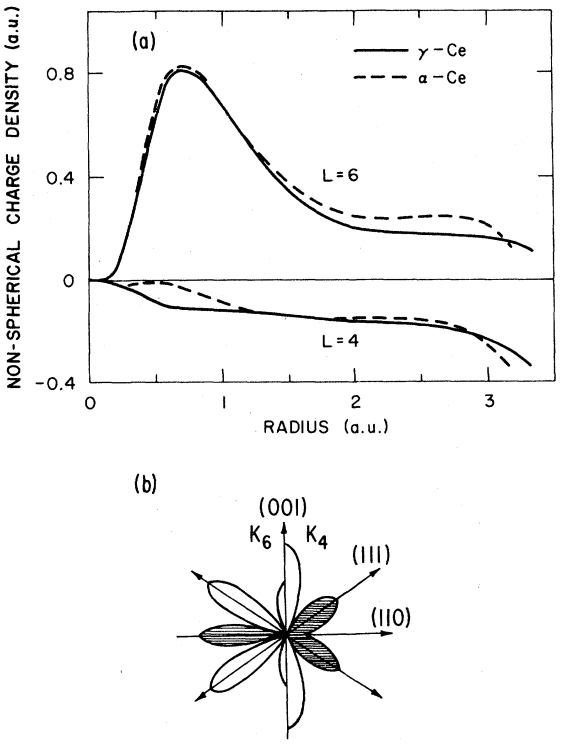

FIG. 10. (a) The nonspherical charge densities for γ-Ce and α-Ce, discussed in the text. (b) The $L=4$ and $L=6$ Kubic harmonics in the $1\bar{1}0$ plane. The cross-hatched lobes denote regions where the harmonics are negative.

for σ bonding. Further, charge is diminished in the [100] directions by the aspherical components; thus, if there is any bonding character at all, it must be of π (or higher) type. The f eigenvalues also reflect this tendency. The lowest-energy eigenvalue, $\Gamma_{2'}$, belongs to a function $\psi(\Gamma_{2'}) \sim xyz$ which points towards the unoccupied region of the fcc unit cell. It is thus able to assume the most "bondinglike" character, e.g., lowest energy, most extended and thus involving the least kinetic energy, without having to actually form an f-f sigma bond which seems to be energetically unfavorable.

The variation of the aspherical terms with lattice constant is readily understood. In the region from $\frac{1}{2}$ to 1 a.u., the increase in size of the $l=4$ component and decrease in the $l=6$ component observed when going from α-Ce to γ-Ce is due to the effect of the decreased $Q(\Gamma_{15})$ seen in Table IV. As the Γ_{15} wave function is strongly directed along a [100] direction [$z(5z^2-3r^2)$ type], this decrease will result in a decrease in the density in that direction. As the peak in the $l=6$ component is directly related to the principal maximum of the f orbital (Fig. 9), one sees that this $l=4$ effect also occurs at that point. The more rapid downturn near $r=3$ is a direct result of the closer proximity of the nearest neighbors. In an fcc metal with no nonspherical single site occupation, both of the Kubic harmonic radial functions would be negative consistent with the overlap of spherical charge densities. As the neighbors are brought closer, this effect is increased. The remaining effect occurs in the region $r > 1.5$ a.u. and can be attributed to the increase in f radial density in that same region shown in Fig. 9. In turn, one should observe that the increase in density in that region is directly related to the increased separation in energy of the f-band center from the Fermi energy.

B. Fermi surface

There are no experimental data on the Fermi surface (FS) dimensions of any phase of Ce available at present, due primarily to difficulties in preparing single crystal, allotropically pure samples. Techniques in sample preparation are improving, however, and so this situation may change soon.

The cross sections of the Fermi surfaces in the symmetry planes are shown in Fig. 11. The cross sections were obtained from a 65-star Fourier series fit to 293 SO-LAPW (LAPW *including* spin-orbit corrections as discussed in Sec. II C) eigenvalues, with an rms error of ~ 3 mRy. It is not sufficient to use the spin-orbitless eigenvalues since relative eigenvalue shifts in the vicinity of E_F due to spin-orbit corrections can be as large as 5 mRy, and the bands often are extremely flat.

It is instructive to compare the FS of Ce with that of Th. Th is at the beginning of the actinide series and, like Ce, has four electrons outside closed shells. Unlike Ce, it has little f-orbital occupation. However, it has been pointed out that the f resonance of Th must be included in order to properly adjust the size of both the Γ-centered "superegg" and the L-centered (triangular) "dumbbell" Fermi surfaces.[43]

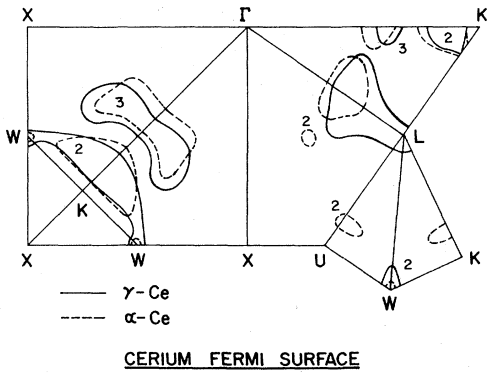

FIG. 11. Fermi surface cross sections in the high-symmetry planes of the γ and α phases of Ce. The changes of topology are discussed in the text.

Further, the nonspherical components of the density show evidence of f-orbital effects as well.

The γ-Ce surface consists of a band 3 electron surface which strongly resembles the "lungs" in Th and a band 2 hole surface at L that is easily identified with the "dumbbells" of Th. (Note that because of the flatness of the bands in this region, the dimensions of this L-centered surface have relatively large uncertainties.) The Th Γ-centered piece is missing in Ce. As this was the piece made smaller by the inclusion of the f orbitals, it is quite reasonable that it should vanish in Ce where the f orbitals are more strongly occupied. Band 2 is an f state at Γ in Ce as can be seen from Table III. The remaining band 2 complicated hole surface in Ce is a multiply connected piece passing through the W points and across the Γ-K line. In Th, band 2 rises very near the Fermi energy at these points giving rise to a peak in the density of states just below E_F. In fact, a small modification of the potential can actually drive these points above E_F.

In going to the α phase, one finds that the electron lungs are little affected, being merely shifted somewhat towards Γ. The dumbbells are squeezed off at L as band 2 drops below E_F. This is an f-orbital effect as band 2 is predominantly an $f(\Gamma_{15})$-type state at L (Table V). It is the occupation of this region around L which gives rise to the increase in Γ_{15} density discussed previously. The multiply connected hole surface simplifies somewhat as it breaks up into a set of small spheroids at the W points together with a still multiply connected surface near K. In addition, a set of small spheroids appear in the ΓLUX plane.

In light of the number of modifications of Fermi surface topology which occur in going from the γ to the α phase, it is interesting to speculate whether there might not be some interesting electronic transition effects of the Lifshitz-Dagens type[42] in the pressure dependence of Ce and the Th-Ce alloy system.

C. Comparison with previous calculations

Various calculations[23,24,31–35] on Ce have demonstrated that self-consistency is crucial for a correct description of the electronic structure, particularly the f-band position. Therefore we will only compare the present results with previous calculations which are self-consistent. This confines the discussion to the early work of Kmetko and Hill[23] and the more recent results of Glötzel.[35]

As mentioned in the Introduction, Glötzel found 1.2 $4f$ electrons in α-Ce, compared to the present result of 1.1 $4f$ electrons. Part of this discrepancy can be ascribed to conflicting definitions of $4f$ charge. With the ASA approach of Glötzel the radial $4f$ function, g_3, extends to the Wigner-Seitz sphere radius R_{WS}. The increase in g_3 between R and R_{WS} can be imagined by continuity of the radial functions pictured in Fig. 9. The contribution to Q_f from the region between R and R_{WS} is of the order of 0.1–0.2 electron, so the calculated $4f$ "occupation numbers" are not necessarily inconsistent. However, these interstitial $4f$ electrons cannot be considered as localized, leading us to expect our value of 1.1 to be a more accurate estimate of the *atomiclike* $4f$ occupation number in α-Ce.

TABLE V. Wave-function character W for band 2 at the high-symmetry points determined from a charge decomposition inside the APW sphere. Note that the states at L and W, which are important in determining the Fermi surface, have considerable $4f$ character.

	Γ		X		L		W		K,U	
	γ-Ce	α-Ce	γ-Ce	α-Ce	γ-Ce	α-Ce	γ-Ce	α-Ce	γ-Ce	α-Ce
$E-E_F$	−3	−12	−98	−150	1	−7	3	3	−20	−29
$W(s)$	· · ·	· · ·	· · ·	· · ·	0.002	0.002	· · ·	· · ·	· · ·	· · ·
$W(p)$	· · ·	· · ·	· · ·	· · ·	· · ·	· · ·	0.035	0.034	0.092	0.081
$W(d\Gamma_{25'})$	· · ·	· · ·	0.776	0.784	· · ·	· · ·	0.215	0.246	0.451	0.418
$W(d\Gamma_{12})$	· · ·	· · ·	· · ·	· · ·	· · ·	· · ·	0.009	0.005	0.110	0.116
$W(f\Gamma_{2'})$	0.914	0.929	· · ·	· · ·	0.111	0.126	· · ·	· · ·	0.001	· · ·
$W(f\Gamma_{25})$	0.045	0.017	· · ·	· · ·	0.031	0.012	0.331	0.346	0.095	0.160
$W(f\Gamma_{15})$	· · ·	· · ·	· · ·	· · ·	0.805	0.791	0.319	0.272	0.015	0.014
$W(g)$	· · ·	· · ·	0.003	0.003	· · ·	· · ·	0.001	0.002	0.004	0.005
W(total)	0.959	0.946	0.779	0.788	0.949	0.931	0.909	0.906	0.766	0.795

Glötzel found $N(E_F)=22.4$ states/Ry spin, which is over 40% larger than we find, and can perhaps be accounted for by a slightly different f-band position relative to E_F. At present the origin of this discrepancy is not clear.

The APW calculations of Kmetko and Hill, though self-consistent, were nonrelativistic. It is well known that relativistic effects lower in energy states with low angular-momentum values, which are relatively closer to the nucleus, with respect to higher l states. This effect appears to be very important in Ce: Kmetko and Hill find an occupied s-band width in γ-Ce of 0.15 Ry compared to our value of 0.25 Ry. A smaller d-f shift (of the order of 0.04 Ry) also occurs, and as a result their value of $Q_f=1.65$ is substantially reduced (to 1.1). However, their conclusion that Q_f changes slowly, and probably insignificantly, as the atomic volume is reduced is supported by our results.

D. Comparison with experiment

Two problems arise in trying to compare our results with experimental data. First, samples below room temperature have not been single phase, and often magnetic impurities are present. Only recently have allotropically pure samples free of magnetic impurities been prepared.[2] Secondly, the lattice constant varies significantly with pressure and temperature in α-Ce, while we have done a single calculation which is appropriate for α-Ce. This lattice constant, 9.0550 a.u. = 4.790 Å, corresponds to 300 K and 20 kbar, or, from thermal expansion and compressibility data,[44] to approximately 15 kbar at $T=0$. Since many aspects of the electronic structure, especially $N(E_F)$, are sensitive to lattice constant, the comparison with experiment given below must be considered somewhat approximate in this context.

1. *Specific heat and magnetic susceptibility*

For the linear specific-heat coefficient γ and the magnetic susceptibility χ we will rely strongly on the overview of Gschneidner[2] concerning the applicability of data (especially the earlier work) to pure Ce. The relation

$$\gamma=(\pi^2/3)k_B^2(1+\lambda_{\rm tot})N(E_F) \tag{5}$$

defines the total specific-heat mass enhancement $\lambda_{\rm tot}=\lambda+\lambda_{ee}$, where λ is the (usually dominant) electron-phonon contribution and λ_{ee} arises from other effective interactions between electrons, often under the name of spin fluctuations, paramagnons, or antiparamagnons. In this section $N(E_F)$ will denote the value for both spins.

For α-Ce Koskimaki and Gschneidner[5] found $\gamma=12.8$ mJ/mole K^2 at ambient pressure, while Phillips *et al.* found 11.3 mJ/mole K^2 at 10 kbar. Extrapolating approximately to $\gamma\simeq 10.5$ mJ/mole K^2 for the lattice constant we have used, $N(E_F)=31.6$ Ry^{-1} atom^{-1} leads to $\lambda_{\rm tot}\simeq 0.9$. We show in Sec. IV that $\lambda\simeq 0.5$ for α-Ce, implying an electron-electron mass enhancement $\lambda_{ee}\simeq 0.4$. This value is comparable to values of[45] $\lambda_{ee}=0.35$ for Pd and 0.2 for Nb,[46] which are among the most firmly established for transition metals. (The recent, much larger, result of Bastide *et al.*[5] for α-Ce gives $\lambda_{ee}\simeq 3$! However, these γ values were extracted from room-temperature data, with the concomitant uncertainties arising from the subtraction of a very large and uncertain phonon contribution to the specific heat.)

For γ-Ce, Gschneidner[47] has analyzed room-temperature data (which is the only possibility for this phase) to find $\gamma=7.5$ mJ/mole K^2. This should be compared to the *itinerant* density of states $N_{\rm it}(E_F)=N(E_F)-N_f(E_F)=14.5$ Ry^{-1} atom^{-1} (Table IV), since the Ce ions are magnetic in this phase. The resulting enhancement $\lambda_{ee}\simeq 1.6$ (recall that $\lambda=0$ at high temperature) may be more reasonable here, where the magnetic, but disordered, f electrons could lead to a very large paramagnon enhancement.

The magnetic susceptibility consists of a number of contributions from the s, p, d, and f electrons and may be written schematically as

$$\chi=\chi_{s,p}+\chi_d(T)+\chi_f(T)+\chi_{\rm VV}+\chi_{\rm dia}\ , \tag{6}$$

where $\chi_{\rm dia}$ is the diamagnetic susceptibility from the core electrons. The first three terms represent the usual paramagnetic spin susceptibility χ_p arising from the conduction-electron density of states at E_F,

$$\chi_p=\mu_B^2 N(E_F)S\ . \tag{7a}$$

The temperature dependence of the high density of states terms has been explicitly indicated in Eq. (6). The Stoner factor S can be written in terms of an (essentially intra-atomic) exchange integral I_{xc} (which includes correlation effects beyond direct exchange[48]) as

$$S=[1-I_{xc}N(E_F)]^{-1}\ . \tag{7b}$$

Kubo and Obata[49] first recognized that the Van Vleck orbital contributions, $\chi_{\rm VV}$, to the paramagnetic susceptibility may be comparable to the spin contribution. Calculations of both the spin contribution[48] and the orbital contribution[49,50] in both simple and transition metals have borne this out. For example, in vanadium[50] $\chi_{\rm VV}$ *is greater than* χ_p. Since we expect large orbital contributions to χ from the open f shell we will account approximately for this by estimating S, and subsequently I, from the relation

$$\chi_p\simeq\tfrac{1}{2}\chi\ . \tag{8}$$

The susceptibility of α-Ce has an unexplained U-shaped behavior[4,51] with temperature, rising much more quickly at low $T(<20$ K) than at high $T(>100$ K). The temperature-independent part can be estimated as $\chi_0 \simeq 5.5\times10^{-4}$ emu/mole at 10 kbar, which with relations (6)–(8) gives $S=3.6$ and $I_{xc}=23$ mRy. Glötzel[35] has *calculated* χ_p for α-Ce, obtaining $S=2.8$, $I_{xc}=14$ mRy (allowing for the factor of 2 difference in his definition of I_{xc}). His value of $\chi_p=3\times10^{-4}$ emu/mole is quite close to our estimate $\chi_p=\frac{1}{2}\chi_0$. His smaller value of I_{xc} may reflect a difference in f-band position relative to E_F, as discussed previously in relation to his 40% larger value of $N(E_F)$. Analyses similar to Eqs. (6) and (7) have been used by other authors[4,52] to suggest that α-Ce is an "exchanged enhanced" metal similar to Pd, for which Janak[48] has calculated $S=4.46$, $I_{xc}=25$ mRy. It should be noted that, in extracting I_{xc} from S, the value of I_{xc} is not very sensitive to S if $S\gtrsim4$, but instead is fixed primarily by $N(E_F)^{-1}$. For example, if Eq. (8) is not used, but rather $\chi_p\simeq\chi_0$ is assumed, S becomes 7.3 but I_{xc} increases only to 27 mRy $[N(E_F)^{-1}=31.6$ mRy].

Koskimaki and Gschneidner[5] and Bastide *et al.*[5] have applied instead the relations

$$\chi_p=\mu_B^2[N_f(E_F)S_f+N_{sd}(E_F)]\ , \tag{9}$$

$$S_f=[1-I_{xc}^f N_f(E_F)]^{-1}\ , \tag{10}$$

assuming only the f-spin susceptibility is enhanced by an f-electron-electron exchange integral I_{xc}^f. If one also uses Eq. (8), this leads to $S_f=5$, $I_{xc}^f=37$ mRy. The difference between I_{xc}^f and I_{xc} results primarily from the use of $N_f(E_F)$, rather than $N(E_F)$, in the expression (10) for S_f.

The susceptibility of γ-Ce is dominated by the Curie-Weiss term but Burr and Ehara[53] have suggested a temperature-independent contribution $\chi_0\simeq1.4\times10^{-6}$ emu/g. Comparing to the itinerant density of states of γ-Ce leads to $S\simeq2.5$, $I_{xc}=39$ mRy. We believe however that the uncertainties, as well as the lack of understanding[48] of the exchange-correlation integral I_{xc} determined from Eq. (7), do not justify the use of the derived values of I_{xc} to ascertain characteristics of the f electrons in α- and γ-Ce. In fact, Janak[48] has noted the trend that I_{xc} depends strongly on the total charge density rather than simply on the valence charge density (or wave functions).

A sharp rise of $\chi(T)$ in α-Ce at low temperature was found in the earlier work of MacPherson *et al.*[4] and Grimberg *et al.*[51] In the more recent work of Koskimaki and Gschneidner[5] on purer samples, the anomaly was found to be much smaller than found earlier, but an unexplained 10% increase in χ below 20 K remained. Such behavior is not explainable in terms of our band-structure results.

The slower rise at higher temperatures, where χ in-

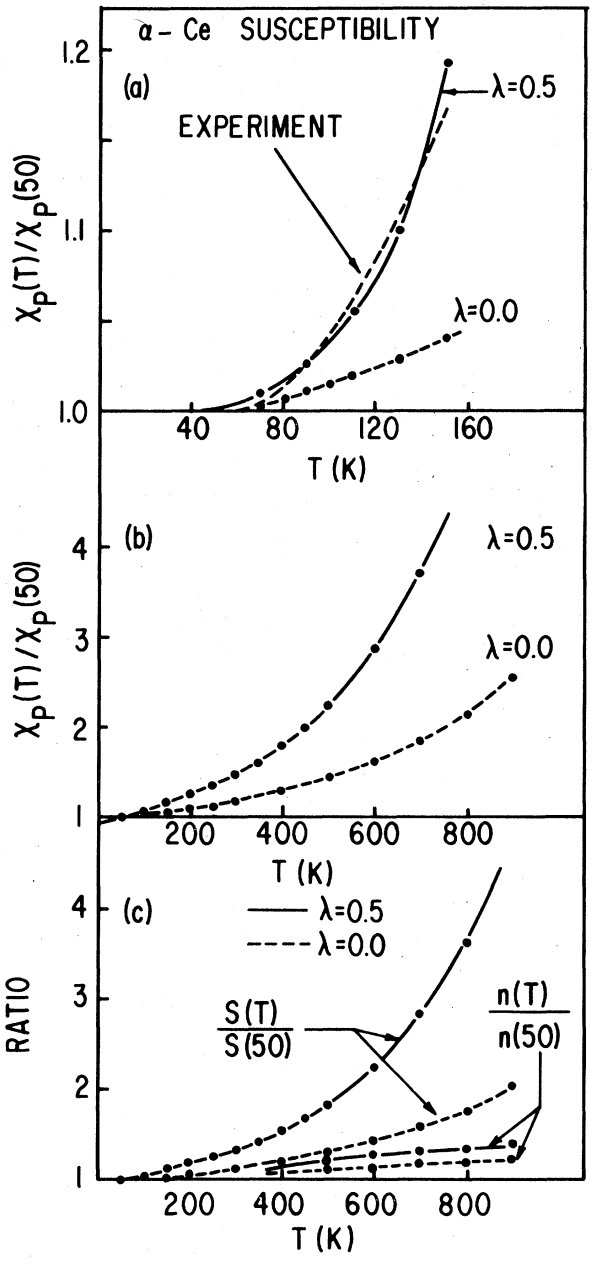

FIG. 12. Calculated temperature dependence of the spin susceptibility of α-Ce, with ($\lambda=0.5$) and without ($\lambda=0.0$) including thermal broadening. (a) The low-temperature region, compared to the experimental result of Koskimaki and Gschneidner (Ref. 5). (b) Temperature dependence up to 900 K. (c) The enhancement $S(T)$ and effective density of states $n(T)$, normalized at 50 K. Note that the increase in the enhancement factor dominates the temperature dependence of the susceptibility.

creases by 15% between 50 and 150 K, may arise from structure in $N(E)$ near E_F. Such an effect has been established in Pd, where χ decreases above 80 K. In α-Ce the proximity of E_F to the huge $4f$ density of states peak would be expected to lead to an increase in χ, as is found experimentally, rather than to a decrease as occurs in Pd. We have calculated the effective density of states $n(T)$ at temperature T from the usual thermal reoccupation expression.

$$n(T)=\int\left[-\frac{\partial f(E-\mu(T))}{\partial E}\right]N(E)dE \quad , \tag{11}$$

where $\mu(T)$ is the chemical potential and f is the Fermi function.

The resulting spin susceptibility

$$\frac{\chi_p(T)}{\chi_p(50)}=\frac{S(T)}{S(50)}\frac{n(T)}{n(50)} \quad , \tag{12}$$

with $S(T)=[1-I_{xc}n(T)]^{-1}$ is compared to experiment in Fig. 12. The theoretical results are normalized to experiment at 50 K, and, as before, we assume $\chi_p \simeq \frac{1}{2}\chi$. In addition we have assumed that the temperature dependence is entirely due to the spin contribution. The calculated increase is about 25% of the measured increase.

A fact that has not been widely recognized is that, in systems where $N(E)$ contains structure on the scale of Θ_D, the effect of the electron-phonon interaction on the spin susceptibility can be appreciable. This effect arises from the *broadening* of the electronic states by the thermal disorder, which results in an effective density of states given by

$$N_{\text{eff}}(E)=\int dE'\frac{(\Gamma/\pi)N(E')}{(E-E')^2+\Gamma^2} \tag{13}$$

and the accompanying shift in the chemical potential, which is used in Eq. (11). We estimate the half-width Γ (which in general will be energy and wave-vector dependent) using the expression from the electron-phonon resistivity

$$\Gamma=\frac{\hbar}{2\tau_{\text{ep}}(T)}=\pi\lambda k_B T, \quad T>\Theta_D \quad , \tag{14}$$

where λ is the electron-phonon coupling constant. This relation, and the value $\lambda=0.5$ which we use, is discussed further in Sec. IV. For $T<\Theta_D$ ($\Theta_D \sim 150$ K) we assume the ideal low-temperature Debye phonon scattering value $\tau_{\text{ep}} \propto T^5$.

The calculated temperature dependence of χ including this thermal broadening of $N(E)$ is also shown in Fig. 12(a). The excellent agreement with experiment may be somewhat fortuitous, since the scale of the "experimental" curve is determined by our assumption $\chi_p \simeq \frac{1}{2}\chi$. However, this assumption is consistent with our determination of I_{xc} above (as it must be) and reasonable deviations from this assumption, as well as small changes in λ or E_F, do not result in any qualitative change in the calculated temperature dependence. In Fig. 12(b) the calculated temperature dependence, with and without thermal broadening, up to 900 K is shown; the $4f$ peak in $N(E)$ makes an *increasingly larger contribution* at higher temperatures. Approximately 80% of the temperature dependence arises through $S(T)$ rather than directly from $n(T)$. This is illustrated in Fig. 12(c), where $S(T)$ and $n(T)$, normalized at 50 K, are plotted.

The enhancement $S(T)$ calculated in this manner in fact *diverges* around 1100 K. We have not considered the implicit temperature dependence of S which arises from the volume dependence of I_{xc} and $N(E)$. However, as the volume increases $N(E)$ generally increases due to band narrowing, and presumably I_{xc} will increase due to increased localization of the valence states. Both of these effects tend to push the divergence of S to *lower temperatures*. This raises the interesting possibility that the magnetic instability $S \rightarrow \infty$ may occur with *increasing* temperature as well as the usual situation which occurs with the lowering of temperature. The requirements for such an instability include a large value of $N(E_F)$ but a *larger* peak in $N(E)$ near E_F. Of course, there is an increasing order-destroying tendency with temperature which opposes this instability. Further experimental work on pure Ce at high temperature would aid greatly in elucidating these conflicting tendencies and their possible connection to the γ-α transition.

2. *Photoemission spectroscopy*

Several ultraviolet and x-ray photoemission spectroscopy studies of Ce have been published.[54–58] The spectra of γ-Ce and α-Ce are similar; there is a general agreement of peaks at binding energies of 1.9 and 1.0 eV (both ± 0.2 eV). The occupied valence bandwidth of 2–2.5 eV in γ-Ce, with a slight increase[57] in α-Ce, is in good agreement with the density of states in Fig. 6. By varying the photon energy Johansson *et al.*[58] were able to establish the 1.9-eV peak as due to the $4f$ state. Platau and Karlsson[55] arrived at the same conclusion using surface-sensitive techniques by showing that this peak is unchanged by oxidation, and hence very localized (nonbonding). The peak at approximately 1.0 eV is interpreted as due to the *sd* valence bands and again agrees well with the density of states peak in γ-Ce (cf. Fig. 6).

The f density of states given in Fig. 8 shows that the local density formalism puts most of the occupied f one-electron eigenvalues within 15 mRy = 0.2 eV of E_F in γ-Ce and within 0.4 eV in α-Ce. However, due to the large occupation number dependence of the f eigenvalues in Ce, the difference between E_F and the f eigenvalues will not correspond to the measured

binding energy. Instead, the binding energy will be increased over the eigenvalue difference by some fraction of the screened intra-atomic Coulomb integral U, the fraction depending on the f occupation number and perhaps the approximate exchange-correlation functional used in the calculation. For Ce, both experimental[58] and theoretical[24] determinations lead to $U \simeq 5$ eV. Implications of a value of U of this size will be discussed further below and in Sec. V.

3. X-ray emission and absorption

The effect of the valence electron configuration on the core eigenvalues has been used by Shaburov *et al.*[59] in an attempt to detect a configuration change in Ce at the γ-α transition. They detected chemical shifts for the K_{α_1}, K_{β_1}, and $K_{\beta_{2,4}}$ x-ray lines of 15, 40, and 9 mRy, respectively, between Ce metal at room temperature and liquid-nitrogen temperature. To infer the configurations of γ- and α-Ce, Shaburov *et al.* performed atomic Hartree-Fock-Slater calculations with Wigner-Seitz boundary conditions. Keeping the configuration $4f^1 5d^1 6s^2$, they found a much smaller chemical shift than seen experimentally. Assuming that α-Ce has the configuration $4f^{0.5}5d^{1.5}6s^2$ led to shifts with the same behavior as seen experimentally, although a factor of 2 too large. Although it was noted[59] that calculational uncertainties (exchange-correlation functional and Latter tail correction) can be as large as 30%, and the magnetic character of γ-Ce and directional bonding of both phases were not taken into account, Shaburov *et al.* concluded that the γ-α transition does involve the promotion of ~ 0.5 f electron.

Our result, that the $4f$ occupation number is unchanged, does not concur with this conclusion. We have found that there is a strong dependence of the chemical shift on the atomic volume of Ce, although the shift *between γ-Ce and α-Ce is indeed small* and consistent with the results of Shaburov *et al.* Our results are summarized in Fig. 13(a), where the eigenvalues involved in the K_{α_1}, K_{β_1}, and K_{β_4} lines are plotted from our crystalline self-consistent calculations at five values of the atomic volume. The experimental results are also pictured in Fig. 13. It is apparent that the chemical shifts can vary strongly (on the scale of the observed shifts) *even though no significant atomic configuration change occurs.* Thus chemical shifts may be sensitive to bonding behavior not directly reflected in the atomic configuration. The parabolic behavior of the chemical shifts of the x-ray lines in Ce is connected with an unusual nonmonotonic behavior (versus lattice constant) of the charge density and potential in the core region. The shift $\Delta E_{\text{core}} = E_{\text{core}}(a_{\gamma\text{-Ce}}) - E_{\text{core}}(a_i)$ in the core

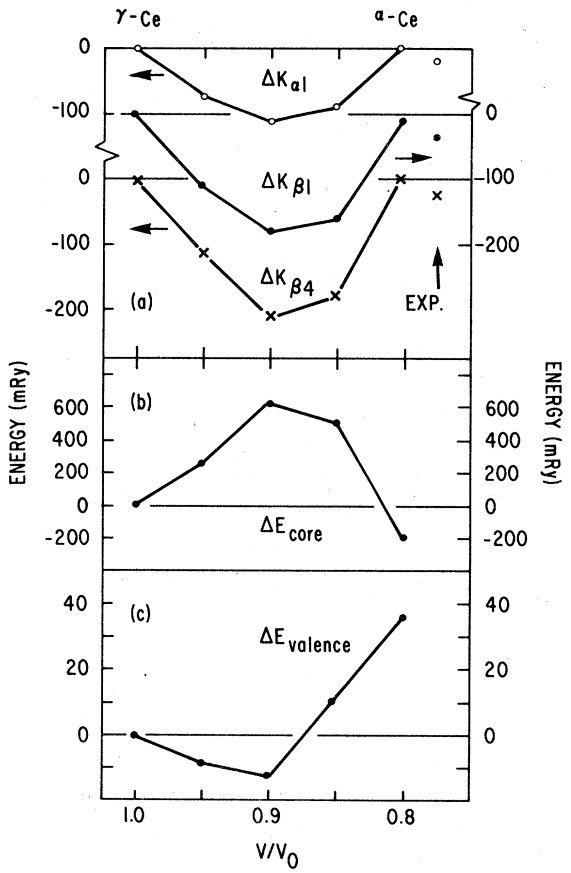

FIG. 13. (a) The differences ΔK_i between the K_{α_1} K_{β_1} and K_{β_4} lines of γ-Ce and Ce at the smaller lattice constants given in Table I. The experimental chemical shift between γ-Ce and α-Ce reported by Shaburov *et al.* (Ref. 59) is shown for comparison. In (b) and (c) the shift in the sum of core and valence eigenvalues, respectively, are shown.

eigenvalue sum $E_{\text{core}} = \sum(\text{core})\ (E_i - E_f)$ is shown in Fig. 13(b) and also shows a parabolic behavior versus lattice constant. The corresponding valence eigenvalue sum, which can be written $E_{\text{valence}} = \int^{E_F} (E - E_F) N(E)\, dE$, is presented in Fig. 13(c) and shows an *opposite* shift, as well as being an order of magnitude smaller. The valence eigenvalue shift is more binding, and the core shift less binding, for the γ and α phases than for intermediate lattice constants. Although we have not yet identified precisely what causes this parabolic behavior, it is likely that subtle but important rearrangements of the $4f$ radial function will be involved.

The effect of the γ-α transition on the $M_{4,5}$ x-ray absorption spectra has been measured by Ottewell *et al.*[60] The differences which were found were interpreted by comparing with the corresponding spectra of "trivalent" CeF_3 and "tetravalent" CeO_2, with the conclusion that their results "provided evidence for

the conversion of tripositive into tetrapositive ions" at the γ-α transition. Until more is known about the electronic structures of CeO_2 and CeF_3, however, this interpretation is open to some dispute. We have not attempted to calculate the $M_{4,5}$ spectra, which is complicated by the need to take into account the correlation energy U.

It is important to include the effect of the magnetic nature of γ-Ce on both emission and absorption spectra; this has not been included in our calculations. The $4f$ radial functions for γ- and α-Ce shown in Fig. 9 would lead to values of U which would differ by less than 5% (by our estimate), barring additional unforeseen differences arising from changes in the metallic screening processes resulting from the varying valence electron density. In an appropriate spin-polarized calculation, the occupied $4f$ state would become somewhat more localized, with a corresponding increase in U. The magnitude of this effect is unknown, but if the change in U is of the order of 1 eV it could account for the effect seen in the $M_{4,5}$ spectra by Ottwell *et al.* The difference in localization of the $4f$ state would also be important in understanding chemical shifts of the x-ray emission lines.

4. *Neutron scattering experiments*

Inelastic neutron scattering[61] from Ce metal at 300 K shows that a dramatic drop in magnetic scattering accompanies the $\gamma \rightarrow \alpha$ transition under pressure. This led to the conclusion that if there is some residual local magnetic $4f$ character in α-Ce, its dynamical response is too weak or diffuse to be observed in the experiment. Further, Stassis *et al.*[62] reported from polarized neutron scattering measurements on single crystal γ-Ce in a polarizing field of 6 T, a field induced $4f$ magnetic form factor in good agreement with that calculated for a Ce^{3+} ion.[63] They also noted suggestions of a reduction of magnetic scattering intensity when the crystal undergoes a transition at 100 K to the α phase. Diffuse neutron scattering measurements on $Ce_{1-x}Th_x$ $(0.2 < x < 0.3)$ have been interpreted as indicating that the full localized $4f$ moment in the γ phase is reduced to 0.4 of that moment in the collapsed phase.[64] This was interpreted as supporting the suggestion that CeTh alloys, like α-Ce, may be configuration fluctuating systems.

Crudely speaking, the experimental data seems to show a magnetic f electron in the γ phase and no magnetic f electron in the α phase. While this interpretation originally appeared to support a promotional model, it is consistent with, and supportive of, a localized-delocalized transformation where the $4f$ electron becomes bandlike and nonmagnetic. We have shown that the $4f$ radial charge density changes appreciably in going from γ-Ce to α-Ce. This delocalization in real space results in a loss of the magnetic moment in α-Ce and so accounts for the observed loss of magnetic scattering.[61,62] The expanded $4f$ radial density would also account for the reduced paramagnetic diffuse cross section in the CeTh alloy.

IV. SUPERCONDUCTIVITY AND TRANSPORT PROPERTIES

When it became evident from specific heat and susceptibility measurements that α-Ce is a very high density of states metal, the question arose as to why it was not a good superconductor, or indeed a superconductor at all. Recently Probst and Wittig[1] found α-Ce to be superconducting at the highest pressures with a maximum T_c of 50 mK and a large pressure derivative $d \ln T_c/dP$. This discovery added to earlier speculation that the apparent exchange enhancement, which would be squeezed out under pressure, was indeed present and adversely affecting superconductivity. In this section we show that the rigid muffin-tin approximation (RMTA) shows α-Ce to be a low T_c metal without invoking other mechanisms. Quantitatively it appears, however, that a small spin-fluctuation contribution is necessary to account for the extremely low value of T_c found experimentally.

A. Rigid muffin-tin approximation

McMillan[65] has shown that the electron-phonon coupling constant λ can be decomposed as

$$\lambda = \frac{N(E_F)\langle I^2\rangle}{M\langle\omega^2\rangle} \equiv \frac{\eta}{M\langle\omega^2\rangle} \ , \tag{15}$$

where $\langle I^2\rangle$ is the mean-square electron-ion matrix element, M is the ionic mass, and $\langle\omega^2\rangle$ is an appropriately defined[65] mean-square phonon frequency. We have evaluated η in the RMTA of Gaspari and Gyorffy[66]

$$\eta = \frac{2E_F}{\pi^2 N(E_F)} \sum_l (l+1)\sin^2(\delta_l - \delta_{l+1})\nu_l\nu_{l+1} \ . \tag{16}$$

Here $\nu_l = N_l(E_F)/N_l^{(1)}(E_F)$, where $N_l^{(1)}(E_F)$ is the "single scatterer" density of states, and δ_l is the phase shift for the lth partial wave scattering from the (spherical) muffin-tin potential. In the RMTA it is assumed that the change in potential when an atom moves is given, in the muffin-tin region, by rigidly displacing the spherical potential, and is zero in the rest of space. This approximation has been used with success in transition metals for calculating T_c (Ref. 67) and the electrical resistivity,[68] which involves similar electron-phonon matrix elements.

It should be noted that Eq. (16) was derived in a

nonrelativistic approximation, whereas the densities of states $N_l(E_F)$ given in Table IV result from a fully relativistic theory. We have not attempted to generalize Eq. (16) to its relativistic analog, but instead have used the calculated $N_l(E_F)$ and the j-weighted average of δ_κ($|\kappa = l$ and $\kappa = -l-1$) for δ_l. The relativistic phase shifts are significantly different for $l=3$($\delta_{\kappa=3}=0.188$ while $\delta_{\kappa=-4}=0.109$ for α-Ce) so relativistic corrections, which we believe to be small, may not be entirely negligible.

In Table VI we list δ_l, ν_l, $\sin^2(\delta_l-\delta_{l+1})$, and the contributions $\eta_{l,l+1}$ to η up to and including the $l=3\leftrightarrow 4$ transitions. The p-d contribution to η is larger than the d-f term, and actually dominates η for α-Ce. This is surprising, since the d-f contribution is the most important one in transition metals and $N_f(E_F)$ is much larger in Ce. The d-f contribution is small for two reasons. First, ν_d and ν_f are small compared to those in high density of states transition metals, the latter being small due to a very large single scatterer density of states—despite the large value of $N_f(E_F)$. Put another way, the large $N_f^{(1)}(E_F)$ prevents $N_f(E_F)$ from canceling the overall factor of $N(E_F)$ in the denominator. Secondly, the same effect that leads to a large $N_f^{(1)}(E_F)$, namely, the proximity of E_F to the $l=3$ resonance, leads to a smaller value of $\sin^2(\delta_2-\delta_3)$ through a larger δ_3. The increase of δ_3 does give rise to a non-negligible small f-g contribution, $\eta_{f,g}$, but this effect is minor.

The volume dependence of the individual contributions $\eta_{l,l+1}$ is illuminating. The d-f (and f-g) term is constant. This is the result of the large changes in $N_f(E_F)$ and $N(E_F)$ canceling out and none of the other parameters changing significantly. On the other hand, $\eta_{s,p}$ and $\eta_{p,d}$ increase strongly upon decreasing the volume. This is primarily due to the decrease in $N(E_F)$ in the denominator, although increases in ν_s and $\sin^2(\delta_1-\delta_2)$ also are important for $\eta_{s,p}$ and $\eta_{p,d}$, respectively.

It has been suggested[69] that f-band metals, with their very narrow bands and high density of states, might provide large values of η and, it is hoped, λ. Our calculations on Ce indicate that this will not occur. An earlier indication of this effect[70] resulted from arbitrarily placing "E_F" in the middle of the f bands of La. This resulted in a much smaller value

TABLE VI. Phase shifts δ_l, density of states ratios ν_l, $\sin^2$ factors, and contributions $\eta_{l,l+1}$ to η(eV/Å^2).

	l	γ-Ce $a=9.7533$	9.5785	9.4040	9.2295	α-Ce 9.0550
δ_l	0	−0.983	−1.019	−1.096	−1.193	−1.234
	1	−0.484	−0.509	−0.560	−0.627	−0.659
	2	0.530	0.552	0.569	0.584	0.604
	3	0.099	0.102	0.119	0.131	0.143
	4	0.0003	0.0003	0.0004	0.0005	0.0005
ν_l	0	1.33	1.55	1.70	1.88	2.30
	1	1.46	1.45	1.30	1.21	1.17
	2	0.71	0.68	0.60	0.55	0.53
	3	2.27	2.16	1.66	1.37	1.28
	4	6.36	6.32	5.15	4.05	4.00
$\sin^2(\delta_l-\delta_{l+1})$	0	0.23	0.24	0.26	0.29	0.30
	1	0.72	0.77	0.83	0.88	0.91
	2	0.18	0.19	0.20	0.19	0.20
	3	0.010	0.010	0.015	0.018	0.020
$\eta_{l,l+1}$	0	0.07	0.10	0.14	0.22	0.29
	1	0.24	0.28	0.30	0.38	0.41
	2	0.14	0.16	0.14	0.14	0.15
	3	0.09	0.11	0.12	0.13	0.15
η		0.54	0.65	0.69	0.87	1.00

of η than was obtained using the actual value of E_F (2.5 eV below the center of the f bands).

Unfortunately, the discussion given above, in terms of the single scatterer density of states, in this case tends to obscure the physical processes which are involved in determining η. Equation (16) can be rewritten, in terms of $\langle I^2 \rangle$, as

$$\langle I^2 \rangle = \sum_l |\langle l | \vec{\nabla} V | l+1 \rangle|^2 f_l f_{l+1} \ , \tag{17}$$

where

$$|\langle l | \vec{\nabla} V | l+1 \rangle|^2 = \left| \sum_{mm'} \int d^3r g_l Y^*_{lm} (\vec{\nabla} V) g_{l+1} Y_{l+1,m'} \right|^2 = \frac{2l+2}{(2l+1)(2l+3)} \frac{\sin^2(\delta_l - \delta_{l+1})}{\tau_l \tau_{l+1}} \tag{18}$$

and

$$\tau_l = \int_0^R r^2 dr \, g_l^2 \ . \tag{19}$$

Equation (17) expresses $\langle I^2 \rangle$ as a squared matrix element coupling l to $l+1$, multiplied by the *fractions* $[f_l = N_l(E_F)/N(E_F)]$ of states at E_F with angular momentum l and $l+1$. The single scatterer density of states is proportional to the normalization integral τ_l of the (nonrelativistic) radial function g_l. Written in this form it is apparent that $\sin^2(\delta_l - \delta_{l+1})$ is dependent only on the *shapes* of the radial functions and their *overlap with* dV/dr. The normalization τ_l, on the other hand, is strongly dependent on the *localization* of g_l. In the Gaspari-Gyorffy[66] formalism $g_l(R)$ is fixed such that the radial function connects continuously with the scattered wave. Thus the radial functions in Fig. 9 are all scaled to (nearly) the same value of $g_l(R)$ in calculating the integrals in Eq. (19). For states which are nearly confined to the muffin-tin region, τ_l becomes very large and their contribution to $\langle I^2 \rangle$ diminishes, reflecting the poor coupling of localized states to scattered waves. Putting E_F in the middle of an f band leads to $f_f \approx 1$, $f_d = \epsilon$, $f_s \approx f_p \approx 0$, giving

$$\langle I^2 \rangle = \epsilon |\langle d | \vec{\nabla} v | f \rangle|^2 \ , \tag{17'}$$

where, in addition to having $\epsilon \ll 1$, the matrix element is very small. The factor $N(E_F)$ multiplying $\langle I^2 \rangle$ roughly cancels the smallness of the matrix element, leaving $\eta \sim \epsilon \to 0$. The values of $\langle I^2 \rangle$, 0.86 $(\text{eV/Å})^2$ for α-Ce and 0.27 $(\text{eV/Å})^2$ for γ-Ce, are among the smallest calculated for any metal to date.

Decreasing the lattice constant from the γ-Ce value to that of α-Ce results in a monotonic, but not necessarily smooth, increase in η from 0.54 to 1.00 eV/Å^2. Glötzel[35] calculated η within the LMTO-ASA approach for α-Ce. In spite of the discrepancy in $N(E_F)$ discussed above, his value $\eta = 1.0$ eV/Å^2 is identical to ours. Previously Mukhopadhyay and Gyorffy[71] considered the magnitude of η in Ce. Although they lacked a self-consistent potential, they were able to show that changing the position of the f bands relative to E_F had a large effect on the resulting value of η. We have shown, however, that localized $4f$ states at E_F will *not* give very large values of η and, within the RMTA, they strongly tend to be detrimental to superconductivity.

B. λ and T_c

In addition to η, the phonon moment $\langle \omega^2 \rangle^{1/2}$ is needed to calculate λ. An additional moment $\omega_{\log}$ is needed as well, since we will calculate T_c from the relation[72]

$$T_c = \frac{\omega_{\log}}{1.2} \exp\left[-\frac{1.04(1+\lambda)}{\lambda - \mu^*(1+0.62\lambda)} \right] \ . \tag{20}$$

The definition of the moments is given by Butler,[67] who has also given the most reliable method of estimating $\langle \omega^2 \rangle^{1/2}$ and $\omega_{\log}$ when detailed information about the phonon spectral function $\alpha^2 F$ is not available. For γ-Ce the phonon dispersion relations have been measured by Stassis *et al.*[73] who also presented the density of states $F(\omega)$, and the corresponding temperature-dependent Debye temperature that resulted from a Born-von Karman force constant representation. For α-Ce, the only information on the phonon spectrum is the low-temperature value of Θ_D, equal to 179 K at ambient pressure and 200 K at 10 kbar.[2,5]

Butler found that Θ_D, which depends only on the $q \simeq 0$ phonons, is not a reliable measure of the phonon moments which are needed. Fortunately, the high-temperature Debye temperature Θ_c (for $T > \frac{1}{3}\Theta_D$), which is an average over the whole spectrum, is more reliable. Specifically, Butler has found $\langle \omega^2 \rangle^{1/2} = 0.69\Theta_c$, $\omega_{\log} = 0.60\Theta_c$ to give good estimates. In[73] γ-Ce, $\Theta_D = 135$ K and $\Theta_c = 117$ K. We will assume that the ratio Θ_c/Θ_D is the same in α-Ce as in γ-Ce.

The calculated values of T_c for γ-Ce and α-Ce, and the constants used in the calculation, are given in Table VII. We have made the usual assumption that $\mu^* = 0.13$ for the Coulomb pseudopotential. The theoretical result $T_c^{\text{theor}} = 1.0$ K for γ-Ce cannot be compared to any experiment, since this phase is not stable at low temperature and, in addition, the magnetic character of this phase has not been taken into account. Nevertheless it will be interesting to use

TABLE VII. Constants needed to calculate T_c for γ-Ce and α-Ce. Phonon moments (Phillips *et al.*, Ref. 5) and experimental value of $T_c = T_c^{\text{expt}}$ (Probst and Wittig, Ref. 1) appropriate for 10 kbar pressure have been used for α-Ce. We have assumed $\mu^* = 0.13$. Comparison with La (Ref. 42) is made in the text.

	γ-Ce	α-Ce	La
$N(E_F)(\text{Ry}^{-1})$	55.1	31.6	13.7
$\eta(\text{eV/Å}^2)$	0.54	1.00	2.62
$\Theta_c(\text{K})$	117	173	
$\langle\omega^2\rangle^{1/2}(\text{K})$	81	119	86
$\omega_{\log}(\text{K})$	70	104	74
$M\langle\omega^2\rangle(\text{eV/Å}^2)$	0.92	1.99	1.84
λ_{theor}	0.58	0.50	1.42
$T_c^{\text{theor}}(\text{K})$	1.0	0.8	8.3
$T_c^{\text{expt}}(\text{K})$	. . .	<0.01	6.05

this value for comparison with the predictions for α-Ce and with those made earlier for La.[42]

For α-Ce (at 10–20 kbar) the RMTA gives $T_c^{\text{theor}} = 0.8$ K whereas $T_c^{\text{expt}} < 0.01$ K. To account for this value of T_c^{expt} using Eq. (20) requires $\lambda_{\text{exp}} \leq 0.30$ rather than $\lambda_{\text{theor}} = 0.55$. It is not possible to reconcile this discrepancy by making *reasonable* changes in the phonon moments ($\sim \pm 10\%$) or in μ^*. For example, $\mu^* = 0.20$ gives $T_c = 0.2$ K, which is still more than an order of magnitude too large. A spin-fluctuation contribution λ_{ee} to the mass enhancement would enter Eq. (20) approximately as

$$T_c = \frac{\omega_{\log}}{1.2} \exp\left[-\frac{1.04(1+\lambda+\lambda_{ee})}{\lambda-\lambda_{ee}-\mu^*(1+0.62\lambda)}\right], \quad (21)$$

with $\lambda_{ee} \sim 0.1$ being sufficient to account for the low T_c in α-Ce. A decrease in λ_{ee} with pressure would also account for the observed rise[1] in T_c, which the increase in the calculated η may not be large enough to account for. [It would be necessary to know the compressibility of α-Ce at low temperature in the range 20–50 kbar to be sure.] Probst and Wittig[1] have suggested lattice softening near the α-α' transition at 50 kbar to account for the rise in T_c in each phase as this phase boundary is approached. There is no direct experimental evidence of this to date, however, and it is difficult to understand why lattice softening with pressure should set in below 20 kbar.

The phonon density of states $F(\omega)$ deduced by Stassis *et al.*[73] corresponds quite closely to the related function $G(\omega)$ for La measured by Nücker.[74] Both spectral functions show a maximum frequency of ~ 12 meV and have corresponding peaks at 10.8 and 8.7 (± 0.2) meV. If the f electron in γ-Ce is assumed to be simply a corelike state screening the nucleus, with negligible dispersion and polarizability, the band structure and phonon spectra of the two materials should be identical. Indeed the phonon spectra are similar, although we believe that in both metals f electron polarizability is important. The band structures at E_F actually differ considerably, of course, and η for La is 2.5 times larger (see Table VII) in spite of a smaller value[42] of $N(E_F)$. The calculated values of T_c differ by an order of magnitude as a result. This provides a vivid example of the detrimental effect of very localized (but still bandlike) f states on superconductivity.

C. Resistivity

The resistivity ρ of α-Ce has been studied by a number of workers,[51,75–78] as a function of temperature and pressure. From the disparity in the measurements it is apparent that $\rho(P,T)$ is very sensitive to the history of the sample and to the method of applying pressure. At present it is not clear how many of the results represent impurity-free, allotropically pure α-Ce. Nevertheless, a short summary of the data is illuminating.

The central question regarding the low-temperature resistivity is the proposed exchange enhancement and the resulting spin-fluctuation resistivity, stimulated by theoretical predictions.[79] Katzman and Mydosh[75] interpreted their results in terms of a *large spin-fluctuation resistivity* and a decreasing exchange enhancement versus pressure. Grimberg *et al.*[51] preferred an interpretation of their data in terms of a *weakly exchange enhanced paramagnet* having pronounced structure in $N(E)$ near E_F. Nicolas-Francillon and Jerome[76] found a *pressure independent resistivity* with a $T^{3.4}$ dependence which they attributed to the electron-phonon interaction. Brodsky and Friddle[77] demonstrated in some detail how important the history of the sample can be for the resistivity.

In samples quenched from room temperature to 77 K, a low-temperature T^2 behavior was found, while for slowly cooled samples an "ideal" electron-phonon T^5 behavior resulted. The samples were cooled at 10 or 18 kbar to avoid the γ-β-α transitions which occur at ambient pressure, but it was concluded that quenching probably induced "magnetic impurities" of β-Ce leading to the T^2 behavior. In any case the existence of samples which obey the T^5 law brings into serious question the earlier identifications of a spin-fluctuation contribution to the resistivity of α-Ce.

For temperatures $140 < T < 300$ K, the resistivity of α-Ce is linear: $\rho(T) = A + BT$. At first sight this behavior appears consistent with Boltzmann's theory, which leads to

$$\rho(T) = \rho_0 + \rho_1 T, \quad T > \Theta_D \ , \tag{22}$$

where $\rho_0 = \rho(T=0)$ is the residual resistivity and ρ_1 is the temperature coefficient arising from the electron-phonon interaction. However, for the data of Brodsky and Friddle,[77] A is not equal to ρ_0 ($\simeq 2$ $\mu\Omega$ cm), but in fact is *negative* ($\simeq -3$ $\mu\Omega$ cm). The data suggest either an alteration in the phonon resistivity (anharmonicity is a likely candidate) or another scattering mechanism, although the apparent lack of any spin-fluctuation (or s-f) contribution at low temperature seems to rule out the most obvious possibility. In any case, the data can be represented by

$$\rho(T) = (\rho_0 + A') + (\rho_1 + B')T, \quad 140 < T < 300 \text{ K} \ . \tag{23}$$

Comparison of the T^5-to-T transition region with ideal Boltzmann-Debye behavior leads to an estimate $\rho_1 T_R \simeq 25$ $\mu\Omega$ cm ($T_R \equiv 300$ K) leaving $B' T_R \simeq 15$ $\mu\Omega$ cm. Using the usual analysis of the electron-phonon resistivity

$$\rho_1 T = 4\pi/[\Omega_p^2 \tau_{ep}(T)] \ , \tag{24}$$

$$\hbar/\tau_{ep}(T) = 2\pi \lambda_{tr} k_B T \ , \tag{25}$$

$$\Omega_p^2 = \tfrac{4}{3}\pi e^2 N(E_F) v^2(E_F) \ , \tag{26}$$

where τ_{ep} is the phonon-limited electron scattering time, $\hbar\Omega_p$ is the "plasma energy," and $v^2(E_F)$ the mean-square Fermi velocity (see Table VIII), we deduce a value for the transport electron-phonon coupling constant $\lambda_{tr} = 0.45$. Therefore $\lambda_{tr} \approx \lambda$ seems to be a reasonable approximation in α-Ce, as has been found previously[68] for transition metals.

D. Thermopower

The room-temperature thermopower Q_T, as measured recently by Khvostantsev and Nikolaev,[80] is positive with magnitude 10 μV/K at ambient pressure. Under pressure Q_T increases to 20 μV/K at the γ-α transition, then decreases rapidly in the α phase to a minimum of 2 μV/K around 25 kbar. At higher pressure Q_T increases slowly until reaching the α-α' transition, where Q_T increases smoothly to a value 8 μV/K over a region of 10–15 kbar.

TABLE VIII. Calculated rms Fermi velocity $v(E_F)$ (in 10^7 cm/sec) and plasma energy $h\Omega_p$ (in eV) for five values of the Ce lattice constant.

a	$v(E_F)$	$h\Omega_p$
9.7533	2.1	3.7
9.5785	2.4	4.1
9.4040	2.6	4.2
9.2295	3.0	4.5
9.0550	3.2	4.7

The thermopower depends sensitively on the electronic structure in a region around E_F. Q_T can be written

$$Q_T = -\frac{\pi^2}{3}\frac{k^2 T}{|e|}\left[\frac{d \ln\sigma(E)}{dE}\right]_{E=\mu} \ , \tag{27}$$

where $\sigma(E)$ is the conductivity calculated as if E were the Fermi energy. We treat σ in two *approximate* ways to try to understand the behavior of Q_T:

$$\sigma(E) = \frac{e^2}{3}\int dE' \left[-\frac{\partial f(E'-E)}{\partial E'}\right] N(E') v^2(E') \tau(E')$$

$$\simeq \frac{e^2}{3}\overline{N\tau}\langle v^2(E)\rangle \ , \tag{28}$$

$$\sigma(E) = \frac{e^2 l}{12\pi^3\hbar} S(E) \ . \tag{29}$$

In Eq. (28) the Fermi surface anisotropy has been averaged out and use is made of the result that the primary energy dependence of τ is given by $\tau(E) \sim [N(E)]^{-1}$. Together with $Q_T > 0$, this expression implies that $v^2(E)$ is a decreasing function of E around E_F. Our calculated $v^2(E)$ values show this behavior, which results from a higher density of flat f bands at higher energy in this range. We find $[d \ln v^2(E)/dE]_{E_F} = -92$ Ry^{-1} and -24 Ry^{-1} in γ-Ce and α-Ce (at 20 kbar), respectively. This value gives

Q_T a value which is too large by a factor of 5, but it is encouraging that the ratios of the γ- and α-phase thermopowers are reproduced. The expression (28) is in any case too oversimplified to expect accurate predictions in a material such as Ce.

In Eq. (29) it is assumed that the mean free path l is independent of energy and wave vector, in which case σ depends on the Fermi surface area $S(E_F)$. From this point of view the peak in Q_T at the γ-α transition suggests a Fermi surface instability for which $[dS(E)/dE]_{E_F}$ is large and negative. The Lifshitz-Dagens instability, mentioned earlier in the discussion on Fermi surfaces, is one of many possible electronic instabilities which could result in this behavior.

V. DISCUSSIONS AND CONCLUSIONS

A. f electron number and valency

Considering the historical entrenchment of the promotional model (PM) and the more recent controversy over the applicability of this model to the γ-α transition, the most significant result of the study is the constancy of the $4f$ occupation number (near unity) through this transition. Although the promotional model has been criticized previously, first by Kmetko and Hill[23] and later by Johansson,[26] the present work represents the first time state-of-the-art microscopic theory has been applied in a detailed manner to test the foundations of this idea. For γ-Ce, which was treated in a nonmagnetic approximation, small refinements might result if its magnetic character were taken into account. For the controversial case of α-Ce, there is little doubt that a narrow but nonmagnetic $4f$ band is essentially occupied by one electron.

This result is consistent with the existing experimental data, which will be summarized below. However, the uncertainty regarding this transition has persisted because the PM also is consistent with most (but, we believe, not all) data. In fact it is difficult to infer with any certainty the f electron number from most experimental data. An example of the dangers which are involved is provided by the incorrect identification of f occupation from lattice parameter regularities, *regularities which were established in systems which had no f electrons.* A similar misidentification from melting point considerations,[81] giving $Q_f = 1.9$ for Ce at high temperature, also gave a similar overestimate[42] for La. The other argument for the PM, the lack of magnetism in α-Ce, can be understood in terms of a Mott localization-delocalization transition if γ-Ce is near the instability.

The PM could be made to reproduce experimental data[21,22] only if the f eigenvalue was within 0.01 eV of E_F with a width of the order of 10^{-2} eV. However, Kmetko and Hill[23] pointed out, and we have confirmed, that the $4f$ states of Ce must have a width of the order of 1 eV. Johansson[26] has since argued from empirical data that $4f$-to-$5d$ promotion involves too large an energy difference to drive the γ-α transition. The photoemission data, which indicate the f electrons are bound by nearly 2 eV, seem to confirm Johansson's arguments. Unless the "mean field" results reported here are (for some unforeseen reason) totally inapplicable to *both* γ-Ce and α-Ce, it is difficult to understand how the PM can apply to this transition.

The utility of the concept of "valency" is also in question. When this concept was introduced it was implicity assumed that neighboring f states did not overlap appreciably and that hybridization of f states with band states could be neglected. Only in such a case could the f electrons be considered not to participate in bonding, which was the explicit assumption. Our results show considerable overlap as well as extensive hybridization broadening of the f density of states, as is clearly shown in Fig. 8. However, the character of f bonding is certainly different from that of the very wide band s-p-d electrons, and in some respects even tends toward nonbonding character. It is not surprising then that, in terms of s-p-d bonding properties, α-Ce *appears* to have 3.5–3.7 bonding electrons, while γ-Ce, with its more localized f electrons, has been identified with 3.1–3.2 bonding electrons. Even if "valency" were to be used only in this sense in metallic systems, it is not clear that such a concept is very useful.

B. Electron correlation and the γ-α transition

While the PM of the γ-α transition is in question, the importance of the intra-atomic correlation energy U is not. U is established, both theoretically and experimentally, to be roughly 5 eV. The accepted methods of trying to understand the implications of strong electron correlation rely on the Anderson or Hubbard models.[82] Unfortunately these models are too restricted to apply directly to the γ-α transition. In the Anderson model, local moment formation on a sharp localized state near the Fermi energy depends critically on hybridization with delocalized states. This model is applicable only to an isolated state whereas we have found that in Ce there is an *intrinsic* $4f$-band width of the order of 1 eV.

The many-band Hubbard model is not well understood although some progress is being made.[37] Within the Hubbard model the ratio U/W is identified as the controlling parameter for a Mott transition. Here W is an appropriate $4f$-band width including hybridization. For a multiband system there is

some question regarding the critical value for that parameter. The importance of our results is in pointing out the large change in this ratio at the γ-α transition: (1) W changes by at least 40% due to the sensitivity of the tail of the $4f$ function to atomic volume; and (2) U remains relatively constant due to the insensitivity of the $4f$ function in the region of the peak to atomic volume. In fact, what variation in U does occur is opposite to that of W, as are corrections arising from the spin polarization of γ-Ce which are not considered here. Thus more refined estimates would lead to an even larger change in U/W at the transition.

Given then that there is a large variation in U/W at the transition, the question remains whether it spans the critical range. The observations of Glötzel[35] suggest this to be the case. Glötzel allowed the possibility of a ferromagnetic state and found it to be favored over the paramagnetic state at densities at and below that of γ-Ce. The probable positive Θ Curie-Weiss form of the susceptibility of γ-Ce and the antiferromagnetism of β-Ce suggest that an antiferromagnetic arrangement (or spin disordered at high enough temperature) would be the actual instability which then would occur at a somewhat higher density than the ferromagnetic one. (Model calculations indeed predict that the antiferromagnetic state should be preferred, although they have been criticized for including only nearest-neighbor interactions which leads to a bias toward antiferromagnetic order.) Once spin imbalance is introduced the spin dependence of the exchange-correlation functionals acts in such a way as to enhance the localization. It seems likely that, as claimed by Glötzel, the treatment of electron correlation within density functional theory is sufficient to account for the γ-α transition in Ce. Further detailed examination of the mechanisms of the instability should prove very interesting. Possibly the ubiquitous instability of the Ce moment in alloys and compounds as a function of density can be understood on a more general basis. These questions can be addressed by theorists with presently available tools and the answers could have widespread implications.

C. Lattice dynamics of Ce

It was pointed out in Sec. IV that the phonon spectrum of γ-Ce has a frequency distribution which is similar to that of La. Such a behavior would be expected if the additional electron in Ce, which goes into the localized $4f$ state, behaves as a core electron and merely screens the extra charge on the nucleus without significantly contributing to the polarization. However, the phonon spectra of both La and γ-Ce are anomalously soft and the resulting large mean-square amplitude of vibration is reflected in their low melting points.

We have suggested earlier[42] for La that virtual transitions into narrow unoccupied f bands lying 2–3 eV above the Fermi level would account for the extra "renormalization" and hence a softer lattice than the other trivalent metals Sc, Y, and Lu. This virtual polarization of the $4f$ states will also occur in Ce, and to somewhat greater degree due to smaller energy denominators. Virtual polarization also has been invoked by Reese, Sinha, and Peterson[83] for the $5f$ states of Th, but to account for the predominance of nearest-neighbor interactions rather than for any softness of the lattice. Stassis *et al.*[73] have found that the nearest-neighbor force constants of γ-Ce are only 40% of those in Th and in addition there is a very important second-neighbor interaction in γ-Ce. This tends to confirm the suggestion[78] that in Th, which lies in the same column of the periodic table as does Ce, it is the spatial *extension* of the $5f$ orbitals which results in the large nearest-neighbor interaction. It is this spatial extension which results in the center of the $5f$ bands lying ~ 0.4 Ry above E_F and gives a much smaller overall renormalization of the phonon spectrum. Again, Stassis *et al.* have noted that, in comparison to Th, γ-Ce is softer than would be expected from the Lindemann homology rule which takes into account the differences in mass, lattice constant, and melting temperatures.

The $T[111]$ phonon branch of γ-Ce is anomalously soft, with the transverse phonon at the L point being a factor of 2 softer than the corresponding phonon in Th. Stassis *et al.*[73] have noted that this soft phonon could be related to the γ-β (fcc-dhcp) transition in Ce. This becomes more provocative in light of our previous study[42] of fcc La, where a remarkably large generalized susceptibility $\chi(\vec{q})$ was found along this direction. Moreover, $\chi(\vec{q})$ was found to have peaks near the wave vectors which would be involved in an fcc-dhcp transformation, a transformation which *also occurs in La* below room temperature. Considering these correlations, it would be especially helpful to have inelastic neutron scattering results on single crystal La, particularly the fcc phase. Unfortunately, although single crystals of dhcp La can be formed above room temperature, the structural transformation from dhcp to fcc seems always to result in two phase samples, so such an experiment may not be possible at present.

Another useful experiment which should be possible is the measurement of the phonon spectrum of α-Ce versus pressure and temperature. This requires expertise in taking a single crystal of γ-Ce around the critical point (see Fig. 1), which may not be prohibitively difficult. A comparison of the phonon spectra on either side of the γ-α transition at room temperature could lead to insights into the nature of this transformation. The study of the spectrum versus pressure at low temperature would show whether the

superconductivity at high pressure is due to phonon softening, or to electronic changes such as the reduction of spin fluctuations. Finally the temperature dependence of the spectrum in α-Ce could be enlightening in a number of respects. It has not been emphasized in the past that α-Ce is extremely anharmonic, a condition which is reflected in the anomalously large thermal expansion.[44] (Note from Fig. 1 that α-Ce must increase by $\sim 15\%$ in volume from room temperature to the critical point, a range of ~ 280 K.) The study of the anharmonicity could be important in understanding α-Ce; conversely, the study of α-Ce could provide useful clues to the properties of highly anharmonic solids. It should be very useful to know the relationship of the localized $4f$ states to the anharmonicity of α-Ce. All of these questions become more pertinent when one considers the known importance of the electron-phonon interaction for mixed valent compounds.[84]

D. Overview of the experimental results

The interpretation of the various experimental data with regard to the valency, or more specifically the $4f$ occupation number, is confusing at best. For photoelectric emission, the spectra from various groups are consistent. The interpretation, that the γ and α phases have a similar number of f electrons bound by ~ 2 eV, is as unambiguous as possible. Although both positron annihilation and Compton profile data have been interpreted in terms of equal numbers of f electrons in the two phases, these interpretations are not conclusive. Calculations of the Compton profile needed for comparison with the data have not been carried out (see note added in proof). Although the interpretation of the angular correlation of annihilation radiation results has been questioned, the total annihilation rate does seem inconsistent with the PM.

We have reasoned above that neither lattice constant nor melting point correlations can be expected to reflect reliably the f electron number. The x-ray emission and absorption results have also been interpreted to support the PM but we have shown in Sec. III that the data are not inconsistent with a nearly constant f electron number. Although x-ray spectroscopy is sensitive to the electronic configuration, it is also sensitive to local bonding characteristics which are not reflected in the configuration. Nevertheless further x-ray work, e.g., for varying lattice constants (with temperature or pressure), could help to understand the α phase and the transition.

The specific heat and susceptibility of α-Ce, although very large, are not inconsistent with a Fermi liquid in which the $4f$ electrons contribute in a band-like manner. It should be mentioned that the correlation energy U can lead to modifications[84] in the usual Fermi liquid expressions for the linear specific-heat coefficient and the susceptibility, but there is no indication that these corrections are large in α-Ce. The low-temperature rise in the susceptibility is not understood at present. The magnitude of the specific heat and the susceptibility, as well as the lack of superconductivity above 50 mK, suggest that important spin-fluctuation contributions to these properties are present. The lack of spin-fluctuation contributions to the resistivity, at least in some samples, complicates this picture, however. A reliable theoretical determination of the importance of spin fluctuations in α-Ce obviously would be of great interest here.

Note added in proof. Calculations of the Compton profile from a self-consistent linearized muffin-tin orbital approach clearly exclude the possibility of the PM of the γ-α transition [R. Podloucky and D. Glötzel, Physica (Utrecht) B (in press)].

ACKNOWLEDGMENTS

The authors would like to acknowledge stimulating discussions with T. Jarlborg. W.E.P. acknowledges helpful conversations on x-ray spectroscopy with D. J. Nagel and illuminating discussions on the state of the theory of Mott transitions with E. N. Economou and B. N. Brandow. This work was supported by the AFOSR, Grant No. 76-2948 and the U.S. Department of Energy.

---

*Permanent address: Naval Research Laboratory, Washington, D. C. 20375.

[1]For α'-Ce, $T_c \simeq 1.5$ K; see J. Wittig, Phys. Rev. Lett. 21, 1250 (1968). In α-Ce, $T_c = 50$ mK at 40 kbar was found by C. Probst and J. Wittig, in *Proceedings of the 14th International Conference on Low Temperature Physics, Otaniemi, 1975,* edited by M. Krusius and M. Vuorio (North-Holland, Amsterdam, 1975), Vol. 5, p. 453.

[2]See discussion and references in K. A. Gschneidner, in *Valence Instabilities and Related Narrow Band Phenomena,* edited by R. D. Parks (Plenum, New York, 1977), p. 89.

[3]E. Ponyatovskii, Sov. Phys. Dokl. 3, 498 (1958); R. I. Beecroft and C. A. Swenson, J. Phys. Chem. Solids, 15, 234 (1960).

[4]M. R. MacPherson, G. E. Everett, D. Wohlleben, and M. B. Maple, Phys. Rev. Lett. 26, 20 (1971); K. A. Gschneidner, Ref. 2.

[5]N. E. Phillips, J. C. Ho, and T. F. Smith, Phys. Lett. 27A, 49 (1968); N. T. Panousis and K. A. Gschneidner, Solid State Commun. 8, 1779 (1970); D. C. Koskimaki and K. A. Gschneidner, Phys. Rev. B 11, 4463 (1975); J. P. Bastide, C. Loriers, H. Massat, and B. Coqblin, in *Rare*

Earths and Actinides 1977, edited by W. D. Corner and B. K. Tanner, IOP Conf. Proc. No. 37 (IOP, Bristol and London, 1978), p. 66.

[6]T. F. Smith, Phys. Rev. Lett. 17, 386 (1966); M. B. Maple, J. Wittig, and K. S. Kim, *ibid.* 23, 1375 (1969).

[7]M. B. Maple and K. S. Kim, Phys. Rev. Lett. 23, 118 (1969).

[8]M. B. Maple and T. F. Smith, Solid State Commun. 7, 515 (1969).

[9]J. G. Huber and M. B. Maple, J. Low Temp. Phys. 3, 537 (1970).

[10]J. M. Lawrence, M. C. Croft, and R. D. Parks, Phys. Rev. Lett. 35, 289 (1975).

[11]C. Y. Huang, J. L. Smith, C. W. Chu, and P. H. Schmidt, in *High-Pressure and Low-Temperature Physics,* edited by C. W. Chu and J. A. Woollam (Plenum, New York, 1978), p. 169.

[12]H. G. Böttjer and K. Winzer, J. Magn. Magn. Mater. 9, 23 (1978).

[13]G. Riblet and K. Winzer, Solid State Commun. 9, 1663 (1971); M. B. Maple, W. A. Fertig, C. A. Mota, L. E. DeLong, D. Wohlleben, and R. Fitzgerald, *ibid.* 11, 829 (1972).

[14]J. G. Huber, W. A. Fertig, and M. B. Maple, Solid State Commun. 15, 453 (1974); W. A. Fertig and M. B. Maple, *ibid.* 23, 105 (1977); S. Ortega, M. Roth, C. Rizzuto, and M. B. Maple, *ibid.* 13, 5 (1973).

[15]W. H. Zachariasen (unpublished) quoted in A. W. Lawson and T. Y. Tang, Phys. Rev. 76, 301 (1949).

[16]L. Pauling (unpublished), quoted in A. F. Schuch and J. H. Sturdivant, J. Chem. Phys. 18, 145 (1950). Pauling had assigned γ-Ce a valence of 3.2 already in 1947; see L. Pauling, J. Am. Chem. Soc. 69, 542 (1947).

[17]In the literature the terms "intermediate valence" and "mixed valence" are often not differentiated. We will use "intermediate valence" to indicate a nonintegral valence and "mixed valence" to indicate a presence of two or more types of ions, each having an integral valence.

[18]K. A. Gschneidner and R. Smoluchowski, J. Less-Common Met. 5, 374 (1963).

[19]E. Franceschi and G. L. Olcese, Phys. Rev. Lett. 22, 1299 (1969); E. King, J. A. Lee, I. R. Harris, and T. F. Smith, Phys. Rev. B 1, 1380 (1970).

[20]W. H. Zachariasen and F. H. Ellinger, Acta Crystallogr. Sect. A 33, 155 (1977).

[21]B. Coqblin and A. Blandin, Adv. Phys. 17, 281 (1968).

[22]R. Ramirez and L. M. Falicov, Phys. Rev. B 3, 1225 (1971).

[23]E. A. Kmetko and H. H. Hill, in *Plutonium 1970 and Other Actinides,* edited by W. N. Miner (AIME, New York, 1970), p. 233; E. A. Kmetko, in Nat. Bur. Stand. Spec. Publ. No. 323, 1971, p. 67.

[24]J. T. Waber and A. C. Larson, in *Proceedings of the 3rd Rare Earth Conference, Clearwater, 1963,* edited by K. S. Vorres (Gordon and Breach, New York, 1964), p. 351; J. T. Waber, D. Liberman, and D. T. Cromer, in *Proceedings of the 4th Rare Earth Research Conference, Phoenix, 1964,* edited by L. Eyring (Gordon and Breach, New York, 1965), p. 187; J. F. Herbst, D. N. Lowy, and R. E. Watson, Phys. Rev. B 6, 1913 (1972); B. N. Cox and P. Lloyd, J. Phys. F 6, 797 (1976); A. Fröman, in *Quantum Science,* edited by J.-L. Calais, O. Groscinski, J. Linderberg, and Y. Öhrn (Plenum, New York, 1976), p. 179; J. F. Herbst, R. E. Watson, and J. W. Wilkins, Phys. Rev. B 13, 1439 (1976); 17, 3089 (1978).

[25]D. R. Gustafson, J. D. McNutt, and L. O. Roellig, Phys. Rev. 183, 435 (1969); R. F. Gempel, D. R. Gustafson, and J. D. Willenberg, Phys. Rev. B 5, 2082 (1972).

[26]B. Johansson, Philos. Mag. 30, 469 (1974); J. Phys. F 7, 877 (1977).

[27]N. F. Mott, Philos. Mag. 6, 287 (1961).

[28]B. Lengeler (private communication); U. Kornstädt, R. Lässer, and B. Lengeler, Phys. Rev. B 21, 1898 (1980).

[29]M. B. Maple *et al.*, Ref. 6; W. A. Fertig and M. B. Maple, Ref. 14.

[30]L. L. Hirst, J. Phys. Chem. Solids 35, 1285 (1974).

[31]J. T. Waber and A. C. Switendick, in *Proceedings of the 5th Rare Earth Research Conference, Ames, Iowa, 1965,* edited by S. Legvold (Clearing House for Federal Scientific and Technical Information, Washington, D.C., 1966), p. 75.

[32]G. Mukhopadhyay and C. K. Majumdar, J. Phys. C 2, 924 (1969); G. Mukhopadhyay, J. Phys. F 2, 450 (1972).

[33]R. S. Rao, C. K. Majumdar, and R. P. Singh, Phys. Rev. B 19, 6274 (1979).

[34]D. Glötzel and L. Fritsche, Phys. Status Solidi B 79, 85 (1977).

[35]D. Glötzel, J. Phys. F 8, L163 (1978).

[36]J. O. Dimmock and A. J. Freeman, Phys. Rev. Lett. 13, 750 (1964); see the review by A. J. Freeman, in *Magnetic Properties of the Rare-Earth Metals,* edited by R. J. Elliot (Plenum, New York, 1972) for a detailed discussion of Coulomb correlation effects for 4*f* electrons and the review by A. J. Freeman and D. D. Koelling, in *The Actinides: Electronic Structure and Related Properties,* edited by A. J. Freeman and J. B. Darby, Jr. (Academic, New York, 1974) for a similar discussion of the same problem for the 5*f* electrons.

[37]S. K. Sinha and A. J. Fedro, J. Phys. (Paris) 40, C4-214 (1979).

[38]D. D. Koelling and B. N. Harmon, J. Phys. C 10, 3107 (1977).

[39]D. D. Koelling and G. O. Arbman, J. Phys. F 5, 2041 (1975).

[40]A. H. MacDonald, W. E. Pickett, and D. D. Koelling, J. Phys. C 13, 2675 (1980).

[41]N. Elyashar and D. D. Koelling, Phys. Rev. B 13, 5362 (1976); 15, 3620 (1977); N. Elyashar, Ph.D. thesis (University of Illinois, Chicago, 1975) (unpublished); relativistic theory is discussed by M. E. Rose, *Relativistic Electron Theory* (Wiley, New York, 1961).

[42]W. E. Pickett, A. J. Freeman, and D. D. Koelling, Phys. Rev. B 22, 2695 (1980); *Superconductivity in d- and f-Band Metals,* edited by H. Suhl and M. B. Maple (Academic, New York, 1980), p. 99.

[43]R. P. Gupta and T. L. Loucks, Phys. Rev. Lett. 22, 458 (1969); Phys. Rev. B 3, 1834 (1971); D. D. Koelling and A. J. Freeman, *ibid.* 12, 5622 (1975).

[44]J. M. Leger, J. P. Bastide, H. Massat, and P. H. Schaufelberger, High Temp. High Pressures 7, 351 (1975). Beecroft and Swenson (Ref. 3) have noted that the thermal expansion at 20 kbar is more than ten times higher than at ambient pressure.

[45]The total mass enhancement $\lambda_{tot}=0.76$ is taken from values of $N(E_F)$ and references to γ in F. M. Mueller, A. J. Freeman, J. O. Dimmock, and A. M. Furdyna, Phys. Rev. B 1, 4617 (1970); T. J. Watson-Yang, B. N. Harmon, and A. J. Freeman, J. Magn. Magn. Mater. 2, 334 (1976).

The electron-phonon contribution $\lambda = 0.41$ has been calculated by F. J. Pinski, P. B. Allen, and W. H. Butler, Phys. Rev. Lett. 41, 431 (1978).

[46]G. W. Crabtree, D. H. Dye, D. P. Karim, D. D. Koelling, and J. B. Ketterson, Phys. Rev. Lett. 42, 390 (1979); H. Rietschel and H. Winter, *ibid.* 43, 1256 (1979).

[47]K. A. Gschneidner, in *Proceedings of the 4th Rare Earth Research Conference, Phoenix, 1964,* edited by L. Eyring (Gordon and Breach, New York, 1965), p. 153.

[48]S. H. Vosko and J. P. Perdew, Can. J. Phys. 53, 1385 (1975); O. Gunnarsson, J. Phys. F 6, 587 (1976); J. F. Janak, Phys. Rev. B 16, 255 (1977); K. L. Liu, A. H. MacDonald, J. M. Daams, S. H. Vosko, and D. D. Koelling, J. Magn. Magn. Mater. 12, 43 (1979); O. K. Andersen, J. Madsen, O. Jepsen, and T. Kollar, Physica (Utrecht) 86–88B, 249 (1977).

[49]R. Kubo and Y. Obata, J. Phys. Soc. Jpn. 11, 547 (1956).

[50]References to most of the calculations of the orbital susceptibility are given in the recent work of M. Yasui and M. Shimizu, J. Phys. F 9, 1652 (1979).

[51]A. J. T. Grimberg, C. J. Schinkel, and A. P. L. M. Zandee, Solid State Commun. 11, 1579 (1972); Koskimaki and Gschneidner, Ref. 5.

[52]A. J. T. Grimberg and C. J. Schinkel, Solid State Commun. 13, 193 (1973).

[53]C. R. Burr and S. Ehara, Phys. Rev. 149, 551 (1966).

[54]Y. Baer and G. Busch, Phys. Rev. Lett. 31, 35 (1973); J. Electron Spectrosc. 5, 611 (1974); Y. Baer and Ch. Zürcher, Phys. Rev. Lett. 39, 956 (1977).

[55]A. Platau and S. E. Karlsson, J. Phys. (Paris) 40, C5-385 (1979); Phys. Rev. B 18, 3820 (1978).

[56]P. Steiner, H. Höchst, and S. Hüfner, J. Phys. F. 7, L145 (1977).

[57]R. A. Pollak, S. P. Kowalczyk, and R. W. Johnson, in *Valence Instabilities and Related Narrow Band Phenomena,* edited by R. D. Parks (Plenum, New York, 1977), p. 463; S. P. Kowalczyk, Ph.D. thesis (unpublished).

[58]C. R. Helms and W. E. Spicer, Appl. Phys. Lett. 21, 237 (1972); J. K. Lang, Y. Baer, and P. A. Cox, Phys. Rev. Lett. 42, 74 (1979); L. I. Johansson, J. W. Allen, T. Gustafsson, I. Lindau, and S. B. M. Hagstrom, Solid State Commun. 28, 53 (1978).

[59]V. A. Shaburov, I. M. Band, A. I. Grushko, T. B. Mezentseva, E. V. Petrovich, Yu. P. Smirnov, A. E. Sovestnov, O. I. Sumbaev, M. B. Trzhaskovskaya, and I. A. Markova, Zh. Eksp. Teor. Fiz. 65, 1157 (1974) [Sov. Phys. JETP 38, 573 (1974)].

[60]D. Ottewell, E. A. Stewardson, and J. E. Wilson, J. Phys. B 6, 2184 (1973).

[61]B. D. Rainford, B. Buras, and B. Lebech, Physica (Utrecht) 86–88B, 41 (1977).

[62]C. Stassis, C.-K. Loong, G. R. K. Kline, O. D. McMasters, and K. A. Gshneidner, J. Appl. Phys. 49, 2113 (1978).

[63]C. Stassis, H. W. Deckman, B. N. Harmon, J. P. Desclaux, and A. J. Freeman, Phys. Rev. B 15, 369 (1977).

[64]A. S. Edelstein, H. R. Child, C. Tranchita, Phys. Rev. Lett. 36, 1332 (1976); C. Stassis, O. D. McMasters, K. A. Gschneidner, and R. M. Nicklow, Phys. Rev. B 19, 5746 (1979).

[65]W. L. McMillan, Phys. Rev. 167, 331 (1968).

[66]G. D. Gaspari and B. L. Gyorffy, Phys. Rev. Lett. 28, 801 (1972).

[67]Representative of RMTA applications are the results of W. H. Butler, Phys. Rev. B 15, 5267 (1977); D. A. Papaconstantopoulos, L. L. Boyer, B. M. Klein, A. R. Williams, V. L. Morruzzi, and J. F. Janak, *ibid.* 15, 4221 (1977).

[68]F. J. Pinski, P. B. Allen, and W. H. Butler, Phys. Rev. Lett. 41, 431 (1978).

[69]W. H. Butler (private communication).

[70]W. E. Pickett (unpublished).

[71]G. Mukhopadhyay and B. L. Gyorffy, J. Phys. F 3, 1373 (1973).

[72]This expression is the low-λ simplification of the Allen-Dynes equation, see P. B. Allen and R. C. Dynes, Phys. Rev. B 12, 905 (1975).

[73]C. Stassis, T. Gould, O. D. McMasters, K. A. Gschneidner, and R. M. Nicklow, Phys. Rev. B 19, 5746 (1979).

[74]N. Nücker, in Prog. Rep. of Teilinstitut Nukleare Festkörperphysik, Inst. f. Angewandte Kernphysik, Ges. f. Kernforschung Karlsruhe, KFK No. 2538 [Prog. Rep. of Nucl. Solid State Physics, Appl. Nucl. Phys. Inst., Soc. Nucl. Phys., Karlsruhe, KFK No. 2538] (1977, unpublished), p.28.

[75]H. Katzman and J. A. Mydosh, Phys. Rev. Lett. 29, 998 (1972).

[76]M. Nicolas-Francillon and D. Jerome, Solid State Commun. 12, 523 (1973).

[77]M. B. Brodsky and R. J. Friddle, Phys. Rev. B 7, 325 (1973).

[78]J. M. Leger, Phys. Lett. 57A, 191 (1976).

[79]A. I. Schindler and M. J. Rice, Phys. Rev. 164, 759 (1967); P. Lederer and D. L. Mills, *ibid.* 165, 837 (1968); A. B. Kaiser and S. Doniach, Int. J. Magn. 1, 11 (1970).

[80]L. G. Khvostantsev and N. A. Nikolaev, Phys. Status Solidi A 51, K57 (1979).

[81]B. T. Matthias, W. H. Zachariasen, G. W. Webb, and J. J. Engelhardt, Phys. Rev. Lett. 18, 781 (1967).

[82]P. W. Anderson, Phys. Rev. 124, 41 (1961); J. Hubbard, Proc. R. Soc. London Ser. A 276, 238 (1963); 277, 237 (1964).

[83]R. A. Reese, S. K. Sinha, and D. T. Peterson, Phys. Rev. B 8, 1332 (1972).

[84]A review of the phenomena and theoretical understanding of mixed valence compounds has been given by C. M. Varma, Rev. Mod. Phys. 48, 219 (1976).